ISTANBUL TECHNICAL UNIVERSITY ★ ENERGY INSTITUTE

ANALYSIS OF REACTIVITY INITIATED ACCIDENTS FOR ITU TRIGA MARK II RESEARCH REACTOR AND THE DEVELOPMENT OF A NEW ANALYSIS CODE

M.Sc. THESIS

Mohammad ALLAF

Energy Science and Technology Division

Energy Science and Technology Programme

Thesis Advisor: Prof. Dr. Üner Çolak

JUNE 2019

ISTANBUL TECHNICAL UNIVERSITY ★ ENERGY INSTITUTE

ANALYSIS OF REACTIVITY INITIATED ACCIDENTS FOR ITU TRIGA MARK II RESEARCH REACTOR AND THE DEVELOPMENT OF A NEW ANALYSIS CODE

M.Sc. THESIS

Mohammad ALLAF

(301161041)

Energy Science and Technology Division

Energy Science and Technology Programme

Thesis Advisor: Prof. Dr. Üner Çolak

JUNE 2019

İSTANBUL TEKNİK ÜNİVERSİTESİ ★ ENERJİ ENSTİTÜSÜ

İTÜ TRİGA MARK II REAKTÖRÜNDE REAKTİVİTE İLE BAŞLATILMIŞ KAZALARIN ANALİZİ VE YENİ ANALİZ KODUNUN GELİŞTİRİLMESİ

YÜKSEK LİSANS TEZİ

Mohammad ALLAF

(301161041)

Enerji Bilim ve Teknoloji Anabilim Dalı

Enerji Bilim ve Teknoloji Programı

Tez Danışmanı: Prof. Dr. Üner Çolak

HAZİRAN 2019

Mohammad ALLAF, a M.Sc. student of ITU Institute of Energy student ID 301161041, successfully defended the thesis entitled "ANALYSIS OF REACTIVITY INITIATED ACCIDENTS FOR ITU TRIGA MARK II RESEARCH REACTOR AND THE DEVELOPMENT OF A NEW ANALYSIS CODE", which he prepared after fulfilling the requirements specified in the associated legislations, before the jury whose signatures are below.

Thesis Advisor :	**Prof. Dr. Üner Çolak** İstanbul Technical University	.....
Jury Members :	**Dr. Lecturer Senem Şentürk Lüle** İstanbul Technical University	.....
	Dr. Levent Özdemir Turkish Atomic Energy Authority	.....

Date of Submission : 03 May 2019
Date of Defense : 12 June 2019

To my beloved Wife and Parents,

FOREWORD

First and foremost, I would like to thank Allah for giving me the strength, knowledge, ability and opportunity. Without his blessings, this achievement would not have been possible.
Special gratitude and thanks to my advisor Prof. Dr. Üner Çolak for his support, knowledge, and time that he shared with me during my M.Sc. degree's journey.
Finally, I would like to dedicate this work to my wife Zhaniya Toktassynova and my parents; Ali Allaf and Reema Zabadnh, who have always supported me and been there for me. Even though sometimes they forget in which educational year I am.

June 2019

Mohammad ALLAF
(Nuclear Engineer)

TABLE OF CONTENTS

Page

ABBREVIATIONS

BWR : Boiling Water Reactor
CFD : Computational Fluid Dynamics
DNBR : Departure from Nucleate Boiling Ratio
LOCA : Loss of Coolant Accident
LOFA : Loss of Flow Accident
MTR : Materials Test Reactor
NB : Nucleate Boiling
PMH : Prompt Moderator Heating
PWR : Pressurized Water Reactor
RIA : Reactivity Initiated Accident
SPERT : Special Power Excursion Reactor Test
SFR : Sodium Fast Reactor
TRIGA : Training and Research Reactor Manufactured by General Atomics
UUTR : University of Utah TRIGA Reactor

NOMENCLATURE

α	: Thermal diffusivity (m^2/s)
α_{fr}	: Void fraction
E_w	: Energy transfer rate through boiling on condensation ($J/m^3.s$)
F_l	: Interfacial drag force on gas phase due to relative motion between
F_w	: Net wall drag force on liquid phase ($N/m^3.s$)
$\dot{m}$	: Mass rate (kg/s)
β_i	: Delayed neutron fraction at *i*-th group
Γ_l	: Gas phase mass creation rate at two phases interface ($kg/m^3.s$)
Γ_w	: Gas phase mass creation rate through boiling or condensation ($kg/m^3.s$)
λ_i	: Decay constant at *i*-th group (1/s)
E_l	: Energy transfer rate at two phases interface ($J/m^3.s$)
A	: Area (m^2)
C_p	: Specific heat capacity (J/kg.K)
d	: Channel width (m)
D_h	: Hydraulic diameter (m)
f	: Friction factor
g	: Gravitational acceleration (m/s^2)
G	: Mass rate flux ($kg/m^2.s$)
h	: Enthalpy (J/kg)
h_c	: Heat transfer coefficient ($W/m^2.K$)
h_{lp}	: Latent heat of vaporization (J/kg)
k	: Thermal conductivity coefficient (W/m.K)
K	: Loss coefficient due to formation change
$N(t)$	: Neutron density ($Particles/m^3$)
p	: Pressure (N/m^2)
$P(t)$	: Power (W) phases ($N/m^3.s$)
Pr	: Prandtl Number
Q, q'''	: Volumetric heat generation (W/m^3)
q''	: Heat flux rate (W/m^2)
R, r	: Radius, radial Distance (m)
Re	: Reynolds Number
$S(t)$	: External neutron source density ($Particles/m^3.s$)
T	: Temperature (°C)
t	: Time (s)
v	: Velocity of vapor fluid (m/s)
z	: Axial Distance (m)
Λ	: Prompt neutron lifetime (s)
μ	: Dynamic viscosity ($N/m^2.s$)
ρ	: Density (kg/m^3)
$\rho(t)$	: Reactivity ($)

Subscripts

c	**:** Coolant
cl	**:** Cladding region
DNB	**:** Departure from nucleate boiling
f	**:** Fuel region
g	**:** Vapor phase
i	**:** Precursors group
l	**:** Liquid phase
NB	**:** Nucleate boiling
ONB	**:** Onset nucleate boiling
SAT	**:** Saturation

LIST OF TABLES

Page

LIST OF FIGURES

ANALYSIS OF REACTIVITY INITIATED ACCIDENTS FOR ITU TRIGA MARK II RESEARCH REACTOR AND THE DEVELOPMENT OF A NEW ANALYSIS CODE

SUMMARY

Safety analyses have been performed in this study on the ITU TRIGA Mark II Research Reactor commissioned in 1979 for different reactivity initiated accidents (RIA) scenarios. The study starts by highlighting the importance of safety analysis and research reactors in nuclear industry, benchmark analysis aspect, the evolution of the computational and numerical modelling methodologies in developing codes for the utilization in safety analysis.

The objective of this study has involved two phases, first phase consists of; a multi-physics model of ITU TRIGA MARK II using EUREKA-2/RR code. This is a known computer code for transient analysis of the neutronic and thermal-hydraulic behavior for safety analysis of severe accident scenarios (i.e., LOFA, RIA, and LOCA). The model has been used for safety analysis of seven different RIA events. The model development has been initiated by adapting the neutronic models developed by MCNP-V for neutronic fluxes determination and Serpent-2 for finding neutronic parameters (such as; decay constants, delayed neutron fractions, etc.) for six and eight groups. However, the EUREKA-2/RR code has fixed set of neutronic parameters related to precursors groups. Thus, no change has taken place to that respect, except for the effective delayed neutron fraction and prompt neutron generation lifetime. Besides, DISSUE, ICETEA, and PREDISCO codes have been utilized to construct the transient EUREKA-2/RR model. Due to the modelling scheme of EUREKA-2/RR, the thermal hydraulic system has been divided into five channels, each has 10 control volumes (segments) that represent the flow and the heat generation. The scenarios are: protected (with a control system delay of 0.1 second) and unprotected RIA with reactivity insertion (dk/k/step); 0.468$/step, 0.935$/step, and 1.872$/step, also unprotected RIA with slow reactivity insertion rate of 1.872$/ (0.5 seconds) and fast protected (control system delay is 0.01 second) for RIA of 1.872$/step.

The second phase consists of; a completely original code developed for TRIGA MARK II with cylindrical fuel type for simulating the RIA scenarios, and the algorithm has been written using MATLAB programming language. The thermal hydraulic system represented by two channels (hot and average) and two dimensions (radial and axial), also the methodologies adapted are as following; pointwise constant function for the solution of point kinetic equations. The code has the freedom in implementing different neutronic parameters of the concerned reactor. Backward fully implicit finite different method has been adapted for solving the governing equations and heat conductivity equation, in order to escape from the stability restriction imposed by other methods, regarding time step size. Furthermore, hydraulic formulas and heat transfer package have been chosen to suit ITU TRIGA MARK II characteristics. The

heat transfer package is able to predict the heat flux and heat transfer coefficient till the subcooled boiling region. The initial fields are solved analytically, which also represent the parameters of steady-state (operational) conditions. Therefore, the TM2-RIA code aims to predict the TRIGA Mark II behaviors during operational and transient accidental scenarios. The analyzed RIA scenarios with reactivity insertions; 0.468$/step, 0.935$/step, and 1.872$/step. Moreover, to investigate the capability of TM2-RIA and the influence of different sets of neutronic parameters, the analyses have been extended for each RIA scenario by implementing three sets of neutronic parameters; the fixed set utilized by EUREKA-2/RR, six groups and eight groups generated by Serpent-2 model of ITU TRIGA MARK II. Keeping in mind that the analyses consider only forced convective cooling.

The safety analyses demonstrated by EUREKA-2/RR model, have shown the influence of reactivity insertion magnitude, the time between each reactivity insertion, automatic scram control and the delay of the scram action. The results have shown that how significant the influence of the reactivity insertion rate can be. For 1.872$/step; peak power reached more than 450 MW, while in case of 0.935$/step and 0.468$/step they reached around 3 MW and 0.7 MW, respectively. The protected cases have shown strong negative net reactivity, causing a sloppy and a fast increase in the DNBR after it reaches its minimum values. This ensures the safety of the reactor for the three investigated reactivity insertions. However, the bigger the magnitude of reactivity insertion is, the lower the influence of the scram becomes, especially at the reactor kinetics starting stages. The influence of scram is hardly noticed in case of 1.872$/step, especially at the longer delay, while in case of short delay 0.01 sec peak power has reached 438 MW. On the other hand, in case of 0.935$/step, the scram influences the power change behavior, where the reactor's power drops within 1 second to power level less than the operational power. Moreover, the difference in reactor's response due to slow reactivity insertion of 1.872$, when it is compared to fast (step) reactivity, has been translated into; time shifting in peak power occurrence (0.35 seconds difference between fast and slow RIA), and a lower magnitude of power (~117 MW).

It has been concluded that the EUREKA-2/RR model ensures safe performance of ITU TRIGA MARK II for all the presented cases, since all values are inside the safety margins addressed by the safety analysis report and other literature sources. It should be kept in mind that the highest cladding surface temperature and minimum DNBR are around 152℃ and 1.19, respectively. That wouldn't violate the safety of the reactor for more conservative safety margins, since the time of their presence is very short. Besides, in all presented scenarios; the power, fuel and cladding temperatures start declining very rapidly afterwards due to the reactivity feedbacks features of TRIGA MARK II till it reaches a quasi-static transient region, where both external and feedback reactivities almost compensate each other.

The analysis carried out using TM2-RIA code have shown promising performance since the expected trends of power, temperatures, and DNBR have been predicted during operational and transient states. The study has shown the influence of segments' size and number in the steady-state's calculations. In addition, the code doesn't fail to simulate ITU TRIGA MARK II for the presented sets of neutronic parameters. These indicate the flexibility and the advantages that TM2-RIA possess comparing to

EUREKA-2/RR in these regards. Furthermore, the results extracted from TM2-RIA ensures the safety of ITU TRIGA MARK II for the unprotected RIA scenario in case of 1.872$/step. Although the minimum DNBR has been (~0.9) in two of the neutronic sets, no critical consequences have been observed due to the very short time of the reactor being at this state. That being said, the code failed to predict the 0.468/$ RIA event smoothly, where unexpected and strong sloppy decrease has been observed after 5 seconds in power behavior. This can be attributed to the adapted point kinetics solution method, therefore, more improvement in that regard should take place in the future.

By the comparison of TM2-RIA and EUREKA-2/RR results, it can be observed that they show fairly good agreement for RIA scenario of 1.872$/step. Although the trends have kept their similarities throughout the full transient time, the gap between the two trends started being more noticeable with time. Investigation of coolant temperature change has been insightful in understanding the reason behind such change in behavior, which leads into change in heat transfer characteristics. This indicates the impact of the different numerical methods adapted in solving the energy equation. Furthermore, the differences between the performance of the two codes, which becomes more obvious at lower magnitude of RIA events. Can be attributed to the effect of many differences in the code's structures (point kinetics solution method, number and size of control volumes and channels that describe the thermal-hydraulic system, initialization, reactivity feedbacks calculations, etc.).

The influence of neutronic parameters of precursors groups investigation is proved to be essential in understanding the impact of the neutronic parameters choice. It also proves how important it is to utilize the correct set that is also compiling with the point kinetics solution method. The results have shown how each set of neutronic parameters influence may vary with respect to the reactivity insertion rate and causing differences in predicting the concerned parameters. This can be seen by calculating the temporal location where the critical values are reached, in some cases time difference is more than 0.5 seconds. Besides, by evaluating the maximum relative differences of concerned variable (whereas the fixed set in EUREKA-2/RR selected as reference), they have been found to be; 6%, 42% and 13%, corresponding to RIA from the lowest to the highest reactivity insertion, respectively.

İTÜ TRİGA MARK II REAKTÖRÜNDE REAKTİVİTE İLE BAŞLATILMIŞ KAZALARIN ANALİZİ VE YENİ ANALİZ KODUNUN GELİŞTİRİLMESİ

ÖZET

Bu çalışmada, farklı RIA (Reactivity Initiated Accident) senaryoları için 1979 yılında işletmeye alınan İTÜ TRIGA Mark II araştırma reaktörünün güvenlik analizleri yapılmıştır. Bu çalışma; nükleer endüstride güvenlik analizinin ve araştırma reaktörlerinin öneminin yanı sıra karşılaştırma analizlerinin, güvenlik analizlerinde kullanılması için kod geliştirmede kullanılan nümerik modelleme metodolojilerinin geliştirilmesinin önemini vurgulamaktadır.

Bu çalışmanın amaçlarından ilki EUREKA-2/RR kodunu kullanarak İTÜ TRIGA Mark II araştırma reaktörünün multifizik modelini oluşturmaktır. Bu kod çeşitli kaza senaryolarının (LOFA, RIA ve LOCA gb.) güvenlik analizini yapmak için nötronik ve termal hidrolik davranışın geçici durum analizlerinde kullanılmaktadır. Bahsedilen model, yedi farklı RIA senaryosunun güvenlik analizi için kullanılmıştır. Modelin geliştirilmesine, nötron akıları için geliştirilen MCNP-V ile nötronik parametreler için geliştirilen Serpent-2 nötronik modellerinin adaptasyonu ile başlanmıştır. Bununla birlikte EUREKA-2/RR kodunda, öncül gruplar için sabit nötronik parametreler kullanılmıştır. Bu nedenle sadece etkin gecikmiş nötron oranı ve ani nötron üretim zamanı hariç kodda bir değişim yapılmamıştır. Ayrıca, geçici durum EUREKA-2/RR modelini oluşturmak için DISSUE, ICETEA ve PREDISCO kodları kullanılmıştır. EUREKA-2/RR kodunun modelleme özelliklerine göre termal hidrolik sistem, her biri akışı ve ısı üretimini temsil eden 10 kontrol hacmine sahip beş kanala bölünmüştür. Analizi yapılan senaryolar: 0,468$/adım, 0,935$//adım ve 1,872$/adım'lık reaktivite girişi (dk/k/adım) ile korunmalı (0,1 saniyelik gecikmeli bir kontrol sistemi ile) ve korunmasız RIA analizi, ayrıca 0,5 saniyede 1,872$/adım'lık korunmasız yavaş reaktivite girişi oranı ve 1,872$/adım'lık korunmalı hızlı reaktivite girişi oranı ile RIA analizi.

Bu çalışmanın ikinci amacı ise RIA senaryolarının simülasyonu için İTÜ TRIGA Mark reaktörüne özgü orijinal bir kod geliştirmektir. Kodun algoritması MATLAB programı kullanılarak yazılmıştır. Termal hidrolik sistem iki kanal (sıcak ve ortalama) ve iki boyut (radyal ve eksenel) ile oluşturulmuştur. Ayrıca metodoloji olarak nokta kinetik denklemlerinin çözümü için nokta tabanlı sabit fonksiyon kullanılmıştır. Kod ilgili reaktör için farklı nötronik parametreleri uygulamak adına uygundur. Zaman aralığına bağlı olarak diğer yöntemlerin getirdiği stabilite kısıtlamasından kaçınmak adına ana denklemleri ve ısı denklemini çözmek için backward implicit (geriye kapalı) sonlu fark yöntemi kullanılmıştır. Hidrolik formüller ve ısı transferi paketi İTÜ TRIGA Mark II araştırma reaktörünün özelliklerine uygun olarak seçilmiştir. Isı transferi paketi, ısı akısını ve ısı iletim katsayısını soğutulmuş kaynama noktasına kadar kendisi belirleyebilmektedir. Normal çalışma koşullarında kullanılan parametreler analitik olarak çözülmüştür. Bu nedenle TM2-RIA kodu, İTÜ TRIGA Mark II araştırma

reaktörünün hem durağan haldeki hem de geçici durum davranışını analiz etmeyi amaçlamaktadır. Reaktivite girişleri (dk/k/adım) ile analiz edilen RIA senaryoları; 0,468$/adım, 0,935$//adım ve 1,872$/adım 'dır. Ayrıca, farklı nötronik parametrelerin etkisini ve TM2-RIA kodunun kapasitesini gözlemlemek adına üç set nötronik parametre uygulanarak analizler her bir RIA senaryosu için genişletilmiştir. Bu parametreler; EUREKA-2/RR kodu tarafından kullanılan ve İTÜ TRIGA Mark II araştırma reaktörünün Serpent-2 modeli ile üretilen 6 ve 8 gruplu nötron parametreleridir.

EUREKA-2/RR modeli ile yapılan güvenlik analizleri, reaktivite girişi değerinin, her reaktivite girişi arasındaki zaman farkının, otomatik ani durdurma kontrolünün ve ani durdurmadaki gecikmenin etkisini göstermiştir. Sonuçlar, reaktivite girişi oranı etkisinin ne kadar önemli olduğunu göstermektedir. 0,935$/adım'lık reaktivite girişi için yaklaşık olarak 3 MW, 0,468$/adım'lık reaktivite girişi için ise 0,7 MW'a ulaşan maksimum güç, 1,872$/adım'lık reaktivite girişi için 450 MW'dan dan yüksek çıkmıştır. Korunmalı reaktivite girişi analizleri, minimum değerine ulaştıktan sonra DNBR'de hızlı bir artışa neden olan negatif reaktivite göstermektedir. Bu durum analiz edilen reaktivite girişleri için reaktörün güvenli olduğunu garantilemektedir. Bununla birlikte özellikle reaktör kinetiğinin başlangıç safhalarında, reaktivite giriş değeri arttıkça ani durdurmanın etkisi azalmaktadır. 0,01 saniyelik kısa gecikmeli durumda maksimum güç 438 MW değerine ulaşırken, özellikle uzun gecikmeli durumlar için 1,872$/adım'lık reaktivite girişinde ani durdurmanın etkisinin çok az olduğu gözlemlenmiştir. Diğer yandan, 0,935$/adım'lık reaktivite girişinde, reaktör gücünün 1 saniyede çalışma gücünden daha az bir değere düştüğü durumda ani durdurmanın etkisinin güç değişiminde etkisi olduğu gözlemlenmiştir. Ayrıca, reaktörün 1,872$'lık yavaş reaktivite girişine tepkisi hızlı reaktivite girişi ile karşılaştırıldığında maksimum güç 0,35 saniye daha gecikmeli meydana gelmektedir ve değeri (~117 MW) daha azdır.

Tüm güvenlik marjinleri güvenlik raporunda ve referans dökümanlarda belirtilen güvenlik limitleri içerisinde kaldığı için EUREKA-2/RR modeli, bahsedilen tüm analizlerde İTÜ TRIGA Mark araştırma reaktörünün güvenliğinin sağlandığını göstermektedir. Maksimum zarf yüzeyi sıcaklığı 152 ℃ ve minimum DNBR değeri 1,19 olarak gözlemlenmiştir. Bu değerler çok kısa süreliğine gözlemlendiği için reactor güvenliği açısından bir sorun teşkil etmemektedir. Ayrıca, analizi yapılan tüm senaryolarda İTÜ TRIGA Mark II araştırma reaktörünün negatif reaktivite besleme özelliklerine istinaden, yakıt ve zarf sıcaklıkları hızlıca düşmeye başlamıştır.

TM2-RIA kodu kullanılarak yapılan analizler, geçici durum ve normal çalışma koşullarında güç, sıcaklık ve DNBR dağılımları için beklenen sonuçları verdiği için gücenilir bir performans göstermiştir. Bu çalışma durağan durumda çalışan reaktör için kontrol hacim boyutunun ve sayısının hesaplamalardaki etkisini göstermektedir. Ayrıca bu kodun, belirtilen nötronik parametreler için İTÜ TRIGA Mark II araştırma reaktörünün simülasyonunda başarılı olduğu gözlemlenmiştir. Bu açıdan TM2-RIA kodu, EUREKA-2/RR kodu ile karşılaştırıldığında daha avantajlıdır. Bunun yanısıra, TM2-RIA kodu 1,872$/adım'lık korunmasız RIA senaryosu için İTÜ TRIGA Mark II araştırma reaktörünün güvenliğinin sağlandığını göstermiştir. İki nötronik parameter seti için DNBR değeri (~0,9) minimuma ulaşmasına rağmen, reaktör bu durumda çok

kısa sürede kaldığı için herhangi bir kritik sonuçla karşılaşılmamıştır. Bununla birlikte kod, 0,468$/adım'lık reaktivite girişinden beş saniye sonra güç davranışında beklenmedik ani düşüşe sebep olarak tutarlı sonuçlar göstermemektedir. Bunun nedeni uygulanan nokta kinetik çözüm yöntemi olabilir, bu nedenle gelecekte yapılacak çalışmalarla kodun geliştirlmesi gerekmektedir.

TM2-RIA ve EUREKA-2/RR kodu sonuçları karşılaştırıldığında, 1,872$/adım'lık reaktivite girişi senaryosu için tutarlı sonuç gösterdileri gözlemlenmiştir. Bununla birlikte, tüm analiz süresi boyunca tutarsızlıklar da gözlemlenmiştir. Soğutucu sıcaklığı değişiminin incelenmesi, ısı iletimi özelliklerinde değişime neden olan böyle bir davranışın arkasındaki nedenleri anlamada etkili olmuştur. Bu durum, enerji denklemlerini çözmede farklı nümerik yöntemlerin etkisini göstermektedir. Bunun yanısıra, düşük değerli RIA olaylarında daha belirgin olan iki kod arasındaki performans farkı kodların yapısındaki; nokta kinetik denklemlerinin çözüm yöntemi, termal hidrolik sistemi tanımlayan kontrol hacimlerinin ve kanalların sayısı ve boyutu, reaktivite besleme hesaplamaları gibi birçok farklılığa bağlanabilir.

Öncül grupların nötronik parametrelerinin etkisinin sorgulanması, nötronik parametre seçiminin önemini anlamada esastır. Bu ayrıca, nokta kinetik denklemlerinin çözümünde kullanılacak doğru nötronik parametre setlerini seçmenin önemini de göstermektedir. Sonuçlar, her nötronik parametrenin etkisinin reaktivite girişi oranlarına göre nasıl değiştiğini göstermektedir. Bu, bazı durumlarda 0,5 saniyeden fazla zaman farkı için kritik değerlerin ulaşıldığı zaman aralığında gözlemlenebilir. Bunun yanısıra, EUREKA-2/RR'de kullanılan sabit nötronik parametre setinin referans alındığı yerde ilgili değişkenin maksimum relatif farklılıkları hesaplanarak en düşük reaktivite girişinden en yüksek reaktivite girişine kadar ilgili RIA için hesaplanan güç farkı sırasıyla; %6, %42 ve %13 olarak bulunmuştur.

1. INTRODUCTION

Multi-Physics safety analysis is a major aspect in the nuclear industry and it has been becoming more and more essential with time advancing. That's due to its critical value in promoting and attracting trust towards the nuclear energy. It is driven by the assurance of an efficient and safe performance of a nuclear reactor. Because of that, a lot of attention has been focused on creating, improving, and implementing new tools to have a robust structure in conducting the safety analyses, both experimentally and numerically. Research reactors became one of the most essential and first steps in strengthening the safety analyses, and verifying conceptual reactor design and safety systems. Not only in the leading countries in nuclear industry, but expanding that to include new members in the nuclear research field worldwide. However, high costs and the lack of technological resources in some cases made conducting experiments a limited option. Therefore, the role of numerical and computational modelling became very focal in the last couple of decades. That's why more focus has been paid in developing and delivering a more reliable multi-physics models, which are able to replicate and predict the behavior of a nuclear reactor. In order to fill the void that is not covered by the experimental means. Since safety analysis mainly concerns the transient behavior of a nuclear reactor post to a severe accident, such as; LOCA, LOFA, RIA, and many others. Therefore, reliable codes must be able to simulate the incidents and the physical behaviors which take place in the reactor during those stages.

That being said, the main challenge in adapting the numerical model is validating it. Because of that, benchmark data and analyses have been carried out in order to examine the numerical model capabilities in simulating the real dynamic behavior of a reactor. Not only in operational conditions but also in accidental scenarios. Research reactors is the main source of the benchmark data when it comes to accident scenarios, since they are designed for their limits to be pushed. Materials Test Reactor (MTR) with power of 10-MW was one of the oldest research reactors to provide set of benchmark data. Besides, the tests which were performed under the program (SPERT) became a very valuable reference. The reactivity insertion tests and self-limiting

reactor power excursion tests were demonstrated in SPERT-III and SPERT-IV, respectively. The SPERT facilities contained small PWR; highly enriched oxide-fueled plate type with water as moderator. The first set of tests presented in [1] which is more related to the current study, considered three initial operation conditions regarding the coolant temperature; cold startup (~21℃), hot startup (~127℃) and (~260℃) and hot standby (~260℃). Whereas, reactivity insertions ranged from 0.5-1.3$ had been applied for operating conditions similar to commercial PWR. The research results showed that the cold startup initial condition was responding to the reactivity insertion rate, mainly due to fuel temperature change (Doppler broadening) with contribution of (85-95%), and no real damaging power excursions was noticed. On the other hand, cases under hot startup conditions showed similar response, but with a higher peak power level in case of the hotter coolant condition case. Even though, none of them made a big difference with the first case, which indicated that the PMH effect played a more significant role in the dynamic response of the reactor with a contribution of (20-35%). However, in the hot standby case a much higher peak power was reached in a shorter time. Keeping in mind that this case was more dependent on the reactivity rate influence than the previously mentioned cases. The same research's data used for testing (benchmarking) both PARET and IREKIN models, the former gave errors within 30%, whereas the latter had a much larger error margin with respect to the experimental data. Despite that, these results don't resemble the current efficiency of computational modelling capabilities, and a lot of improvements have taken place since then.

The second set of tests presented in [2] involved a stepwise excess reactivity insertion was considered, while short to relatively long periods and no forced to forced cooling (hydraulic conditions) influences had been investigated. It was concluded that the forced convection impact causes higher peak power and power bursts, which was more observable in a long period interval by having a more random oscillatory behavior.

These two sets benchmark data became a reference for many works to come since then related to codes validation. One of these works is presented by Margulis and Gilad [3], in which the SPERT-IV tests had been highlighted and used for benchmark analysis of a new two phase model introduced in this work for THERMO code, through a coupled system (neutronic and thermal-hydraulic) of Serpent and THERMO codes. The results showed that the model is unable to predict the temperature distribution in

the reactivity insertion rates (0.88-1.14$). The power was predicted fairly good at 0.88$ but not with high mass flow rate, although the power and temperature trends were correctly extracted. Therefore, it was concluded from the research that the first form of the two-phase model cannot be recommended and more advanced work need to be done to improve the two phase model. Dokhane et al. [4] performed validation of CASMO/SIMULATE-3K models against the benchmark data extracted in [1] for cold startup case. In addition, the work conducted uncertainty analysis in which it showed that most of the analysis concerned the power, reactivity, fuel temperature and enthalpy were in good agreement with the experimental result. However, slight deviations occurred but due to the small time zone they take place in, that doesn't eliminate the validity of the presented models. However, the models should simulate further scenarios to justify their reliability, since only the cold startup case was concerned.

The issue with benchmark analysis is that not all data falls for all reactors. For example; the data introduced in [1] and [2] are specific to the properties of the reactors that are similar to the PWR that has been tested, when it comes to geometry of the core, fuel material composition, flow mass, etc. They are not valid for BWR or some type of research reactors. Hence, not all codes meant to have the same level of reliability to simulate or model any reactor. There are many parameters play role in defining modelling code scheme; approach in defining the system, i.e. sub-channel as the case in COBRA [5], closed channel as in EUREKA [6] and PARET [7], the spatial dimensions, for steady-state (i.e., COOLOD-N2 [8]) or transient analyses (EUREKA), fuel and cladding geometry and materials type, which equations are considered to be solved and the numerical methodologies adapted in solving the equations, heat transfer correlations package, etc. That being said, all experiments no matter what type of reactor it concerns can help in building a common sense on understanding the behavior in nuclear reactor. Because of that, many works considered benchmarking or verifying their numerical codes using code to code comparison approach, while some depended on creating models through the well-known used codes.

PARET/ANL and RELAP5/MOD3 were benchmarked with the SPERT-IV benchmark data, and the performance of the codes compared against each other by Woodruff et al. [9], the results had shown fairly good agreement. However, RELAP5/MOD3 was modified than its original version when it comes to heat transfer

correlations by utilizing a more reliable correlation for single phase flow in research reactors (Petukhov correlation, where the original version considered Seider-Tate correlation).

Heat transfer correlations (CHF or heat transfer coefficient) play huge role in the thermal hydraulic behavior of a flow in reactor, which correspondingly cause deviations in the safety parameters such as DNBR, surface temperature and other related parameters. The reason behind that is all heat transfer coefficients are empirically defined. Thelera and Freisb [10] adapted the theory proposed by Schroeder-Richter and Bartsch [11] and compared it with Chen's correlation, the developed function produced some promising results, but still the CHF was overestimated.

Furthermore, Guo et al., established RELAP5/MOD3 model for JRR-3MW research reactor was developed to simulate the consequences of LOFA occurrence [12]. It was concluded that departure from nucleate boiling occurred at flow blockage fraction of 50%, but the RELAP model wasn't able to predict the complicated two-phase flow behavior. A further study was presented in [13], it showed how the 3D-detailed model developed by CFD code FLUENT was able to resemble the physical phenomena better than the RELAP model. But both models couldn't accurately predict the behavior of the reactor and when DNB takes place. The last three highlighted studies reflected how RELAP5/MOD3 lacks the correct set of heat transfer correlations that are suitable for research reactors.

On the other hand, PARET/ANL is more commonly used in modelling research reactors, since basically it is designed to simulate the thermal-hydraulic behavior in a nuclear research reactor. Boulaich et al. [14] and Babitz [15] had utilized PARET code in safety analysis; the first study ensured the safety of the TRIGA Mark II during RIA events while scram considered, while the latter simulated the operating condition and ensured the safety of the UUTR.

EUREKA-2/RR is another common and proved to be a reliable code in predicting the behavior of research accidents for safety analysis. The code was used by Badrun et al., to model TRIGA Mark II 3MW research reactor during operational state [16]. It produced close results to the PARET and COOLOD-N2 models developed and benchmarked in previous works for the same reactor. The model then used for simulating the transient behavior of the reactor during LOFA and RIA accidents; in

which the profiles of DNBR, fuel, cladding temperature, power, flow rate, reactivity and reactivity feedbacks were all extracted and proved the safety of the reactor during those events. The safety of the reactor was also justified by the agreement of the results with the safety report addressed in the work. This strengthened the confidence in adapting the EUREKA model in further studies presented in [17] and [18], where unprotected analysis for RIA and LOFA were conducted (unprotected analysis means no scram action was considered), respectively. In the first study the results showed how Doppler effect in TRIGA Mark II helps in sustaining the reactor operates safely, even though the cladding temperature was exceeded but for very short time, hence, the reactor considered safe through the concerned event (till 2.0% dk/k). On the contrary, the second study found departure from nucleate boiling occurrence, hence, the reactor wasn't considered safe at that stage (for 85% loss of flow). The previously mentioned reactor was a cylindrical fuel type reactor, and similar studies on the fuel plate type JRR-3MW and KUR low-enriched Uranium silicide fuel core research reactors were conducted by Kaminaga [19] and Shen et al. [20]. That shows how the code performs well in a wider range of reactor types and scenarios.

It was highlighted in [21] some of safety analysis works that had taken place prior to the studies date related to research reactors, also proposed various research topics to be further considered regarding research reactors multi-physics analyses.

The current study doesn't only concern the utilization and modelling of a reactor transient behavior using a common code. Since as mentioned before codes may not be always suitable for the study case, and usually they need a lot of time and skills to master. Thus, the current study goes even further in the development of a specific multi-physics model for TRIGA Mark II research reactor using different numerical methodologies, correlations and algorithms. Therefore, it is worthy to highlight some similar works and discuss the scheme that was adapted. The model introduced by Housiadas [22] is a very simplified model, where the whole nuclear reactor was lumped into one control volume coupled with point kinetics equations, whereas only fuel and coolant temperatures embody the temperature distribution. The model is very simple to implement, however, the model was only testified for a slow insertion rate and for less than (1.5$/0.5 second). Besides, the results showed a significant deviation in comparison with more detailed models. Similar approach was taken in the model proposed by Kazeminejad [23], however, the code was developed for LOFA analysis,

where a flow inversion model was introduced. The model was applicable only for long period LOFA, since only single-phase flow was modelled. While in the model introduced by Margulis and Gilad [24], the point kinetics and the heat transfer equations were solved using explicit forward finite difference method for a fully lumped, single channel, two channel, and full core. Also 4 different heat transfer coefficient correlations were considered, the correlations caused a difference of almost 80℃ in the peak cladding temperature, which supports what was previously mentioned. The correlation Sleicher-Rouse was found to be with the best estimate, so it was adapted for the code. In general, the code results showed fair agreement with RELAP5 and PARET, however, the results didn't show long time transient behavior, the full presented analyses time was 1.5 second. This brings a question on how much computational time the simulation consumes and whether the code fails in the longer stages. The RETRAC-PC code presented and benchmarked for MTR research reactor by Bousbia-Salah and Hamidouche [25], solves the point kinetics using the modified Rung-Kutta method. Besides, it is based on one-dimensional thermal-hydraulic system and the governing equations are solved using first order finite difference method. The code benchmarked good with the PARET/ANL code, however, with other codes like EUREKA and COBRA it showed a lot of inconsistency in accuracy. The model in [23] was further enhanced by converting the system into 2 channel and introducing a two-phase flow model, where the governing equations are solved using implicit finite difference method [26]. Besides, the heat conductivity equations solved in a two-dimension system using orthogonal collocation method for horizontal direction, central finite difference for axial direction, and the temporal steps solved by forward finite difference. This model was tested for RIA events in a wide range for MTR, the results showed good agreement in general and promising performance. Similar steps were taken by Mazumdar et al. [27], but Crank Nicolson method was adapted in this model scheme. No governing equations considered (the coolant temperature was included in the heat conductivity equation), and point kinetics was solved using piecewise constant function. Some obvious shifting in locating the peaks power, despite that, good agreement was shown throughout the analyses, but the model was valid only for fuel plate type and sub-cooled boiling regime. El-Morshedy [28] developed a model for cylindrical type of fuel elements, the model solved the steady-state heat conductivity equation, then the transient state using implicit finite difference method. However, the model doesn't solve the neutronic equations and consider

reactivity changes, besides, the model wasn't benchmarked with different experimental data or numerical models.

Other works considered developing a coupling scheme between two well-known codes, such as the work presented by Henry et al. [29], in which coupling was performed between the Monte-Carlo TRIPOLI code and the CFD code CFX. The code used for analyzing the TRIGA Mark II in Jozef Stefan Institute, the results was compared to experimental data obtained during operational state. Good agreement was found in general in extracting the bulk temperature at the sensor positions (axially and radially), moreover, the calculations gave promising reliability in predicting the velocity profile in the core. Besides, the study showed the difference between coupled and non-coupled computational results can be considered negligible. That being said, the coupling scheme needs to overcome many challenges to make a transient solution possible, due to the adaptation of Monte-Carlo code.

Moreover, this type of works is not exclusive for research reactors or the current reactors. In fact, there are many works that consider G-IV reactors which are more challenging, due to the lack of benchmark data and the complexity of the flow behavior in some cases. Some of these works were proposed by; Chen et al. [30] for the Chinese Super-Critical Water Cooled Reactor, Sun et al. [31] and Hellesen et al. [32] for Fast Sodium Cooled Reactor types. Which indicate the importance of computational modelling for innovative purposes, and introducing new design concepts that are not applicable at the current time. Furthermore, an attempt in extending SCANAIR code to cover analysis of RIA for BWR was proposed by Arkoma [33], where coupling between two thermal hydraulic codes SCANAIR and GENFLO was proposed. That was done in order to cover a wider range of boiling conditions in bulk region. The attempt showed promising performance, however, there are works need to be done to improve the accuracy of the predictions.

The aim in the current work is to analyze the safety of ITU TRIGA Mark II research reactor prior and post to RIA event, for forced convective cooling. The study involves two stages, first; a multi-physics model is developed using EUREKA-2/RR code, several protected and unprotected (with or without scram system) RIA scenarios are analyzed, the effect of time, reactivity insertion rate and scram system on the transient behavior of ITU TRIGA Mark II are investigated. Second stage; introduces the development of an original unique code for building a multi-physics model of ITU

TRIGA Mark II, which is used to conduct analysis of operational state and RIA scenarios. Finally, investigation of the implemented neutronic parameters' impact and comparison between the two codes' models have been conducted.

1.1 ITU TRIGA Mark II

The reactor ITU TRIGA Mark II was established in 1979. The same year in which operation for the first criticality experiment was performed. The reactor facility is part of the Energy Institute site located in Istanbul Technical University campus. The aim of the reactor is for research, training, and education purposes to demonstrate both steady state and pulsing operations. The reactor has been used for more than 30 years in the following missions:

- To perform experiments related to neutron scattering, radiography, and neutron activation analysis.
- To perform training and education in reactor physics, and mastering the basic principles in operating the reactor.

The reactor core is arranged in a circular array consists of five rings around the central thimble, which provides 90 positions in total for the placement of different elements. Table 1.1 and Figure 1.1 provide the information related to the number and type of elements that allocate those 90 locations. Besides, the reflector material is Graphite, in addition, the reactor consists of three beam ports; radial, tangential and piercing.

Table 1.1 : Number of elements corresponding to its type.

Element Type	Number
Fuel Elements	69
Graphite Dummies	16
Control Rods	3
Neutron Source	1
Pneumatic Hole	1

Each fuel rod (active region) consists of a central Zirconium rod surrounded by a fuel meat which is a homogenized mixture of Uranium (U) and Zirconium Hydride (ZrH1.6) containing 8.45 wt % enriched U having no more than 20% U-235, top and bottom graphite reflectors, the end-fittings and the cladding surrounding the fuel

elements are made of Stainless-Steel (type 304). For better understanding, a relative representation of the fuel element design can be found in [34]. On the other hand, graphite dummies don't contain any fuel and Zirconium compositions, however, they have similar geometry but with Aluminum cladding.

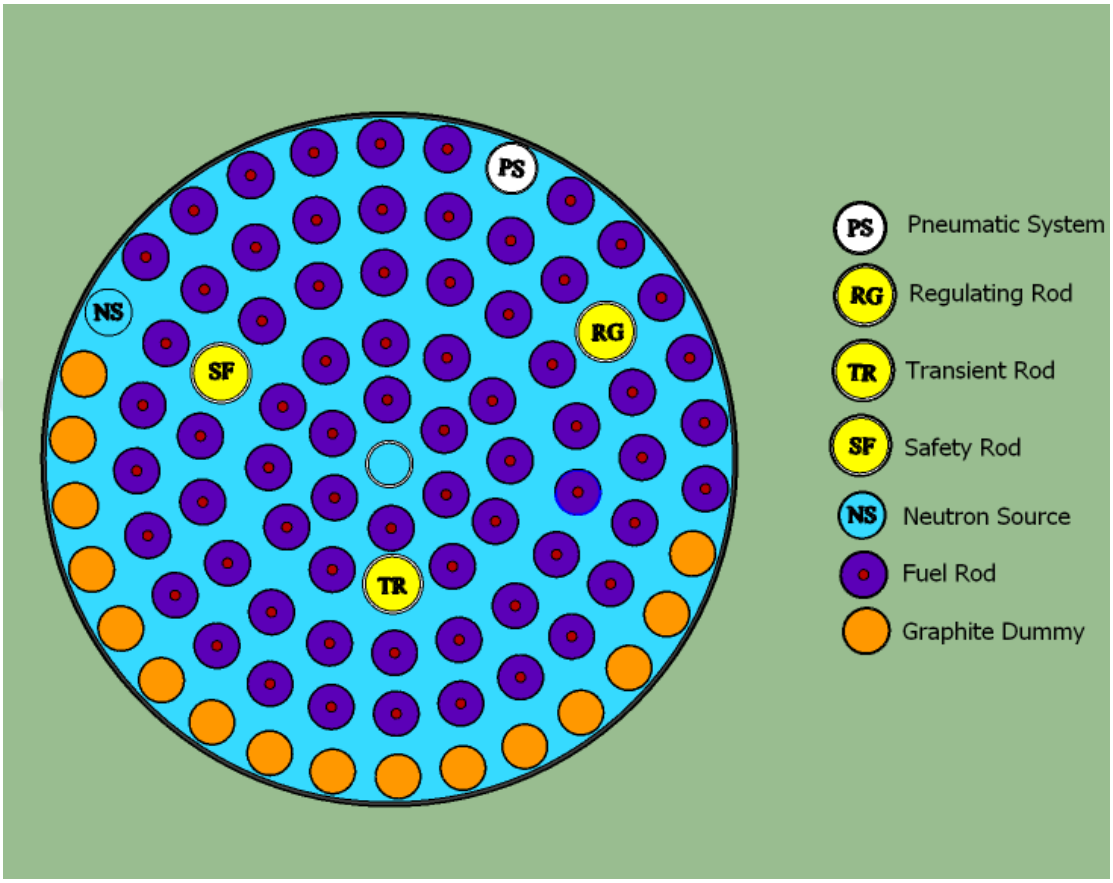

Figure 1.1 : Allocations of elements in core shown in a radial cross-sectional view of ITU TRIGA Mark II.

The three control rods in the core are: transient, safety (shim), and regulating. The functions of these control rods can be defined as following; transient rod is used for power pulses and safety measures, while safety rod is used for coarse reactivity adjustment, finally the regulating rod is used for multiplication factor tuning.

The water flow passes through the holes distributed in the upper and the lower grids, each grid contains 90 holes. Table 1.2 presents important design and thermal-hydraulic parameters and other properties.

Table 1.2 : Characteristics of ITU TRIGA Mark II, [35].

Parameters	Value
Power:	
Steady-State	250 (kW)
Peak power at pulse mode	1200 (MW)
Dimensions:	
Zirconium Rod Radius	0.3175 (cm)
Fuel Rod Radius	1.8161 (cm)
Fuel + Cladding Rod Radius	1.8669 (cm)
Active Height	38.1 (cm)
Hole Radius (in grid)	0.9525 (cm)
Thermal-Hydraulic Parameters:	
Flow Area (per element)	0.000539 (m^2)
Wetted Perimeter (per element)	0.11768 (m)
Hydraulic Diameter	0.018318 (m)
Inlet Coolant Temperature	35(℃)
Heat Surface	3.08216 (m^2)
Materials Properties:	
Density (g/cm^3)	
Fuel	5.828
Cladding	7.94
Specific Heat Capacity W/(kg.℃)	
Fuel	497.47
Cladding	250.236
Thermal conductivity W/(m.℃)	
Fuel	Temperature (0-300) (℃) = 17.5799 Temperature (300-600) (℃) = 19.8303 Temperature (600-1000) (℃) = 21.3294 Temperature (>1000) (℃) = 23.0794
Cladding	16.15407
Velocity (ref. [16])	
For forced convection	2.875 m/s
For natural convection	0.3048 m/s

2. THEORY

2.1 Multi-Physics Model for Nuclear Reactor Analyses

Scheme to simulate and predict the thermal-hydraulic behavior in nuclear reactors; depends on solving and linking the point kinetics solution with the thermal-hydraulic equations, represented by the thermal heat conductivity equation and the governing equations.

The point kinetics equations are described as;

$$\frac{dn(t)}{dt} = \frac{\rho(t) - \beta_{eff}}{\Lambda} n(t) + \sum_{i=1}^{g} \lambda_i C_i(t) + S(t) \tag{2.1}$$

$$\frac{dC_i(t)}{dt} = \frac{\beta_i}{\Lambda} n(t) - \lambda_i C_i(t) \tag{2.2}$$

It is worth mentioning that one of the main feature of the above equations is stiffness, which means that these equations are slow to be solved numerically (the temporal step size must very small). That's why a lot of attempts can be found in literature presenting different numerical methodologies to solve the point kinetics equations. Therefore, it is expected that the finite difference method is quite unsuitable approach for solving these equations. This was proven by Szeligowski [36], by showing how time step size must be very small in order to get the necessary results, which also leads to excessive computing time. The same work compared different methods; a simplified version of Cohen (non-simplified version is adapted in RELAP and PARET codes), Adler, and Collocation methods. It was found that in relatively big time steps, Collocation method was more stable and faster to converge in comparison to the other methods. However, it wasn't consistent in its performance for different reactivity periods, whereas Adler's showed better performance.

Sanchez [37] proposed a Generalized Rung-Kutta (GRK) method to solve the stiffness issue, it was shown to be relatively simple and fast, it was even mentioned the promising capability of this method in solving a space-dependent system. The issue

with this approach is that the proposed solution is A(α)-Stable Rung-Kutta method, and the allowed tolerance in error plays a role in changing the associated constants to the solution [38]. Hence, new set of constants might be required to be generated, which makes the approach only simply applicable for specific time steps and tolerance values that are tested in different works. Taylor series method proposed by Nahla [39], showed better performance than (GRK) for negative step, ramp and reactivity feedback due to temperature. However, further modification and testing are required, to understand the range of its applicability. Chen et al. [40] adapted the singularly perturbed method to solve the kinetics equations, where the neutronic flux solution consisted of two solution parts; inner and outer. The solution was compared against the solution using temperature prompt jump, precursors prompt jump, power prompt jump, and small parameter methods. it agreed very well with the first method and showed much better accuracy in comparison to the others. However, the study considered reactivity insertion rate less than $dk/k/step = 0.0065/step$, thus, it should be tested for a higher magnitude of insertion rate, to evaluate its reliability. Piecewise constant function method proposed by Kinard [41], showed much more efficient solution, when combining the simplicity of implementation, time step size and accuracy, it even produces error of order (Δt^2).

The generic forms of the transient governing equations of a multi-dimensional two phase flow system can be described as introduced by Singh et al. [42];

Mass conservation (continuity) equation:

$$\frac{\partial\left(\alpha_{fr}\rho_g\right)}{\partial t}+\nabla\left(\alpha_{fr}\rho_g v_g\right)=\Gamma_1+\Gamma_w \tag{2.3}$$

$$\frac{\partial\left(\left(1-\alpha_{fr}\right)\rho_l\right)}{\partial t}+\nabla\left(\left(1-\alpha_{fr}\right)\rho_l v_l\right)=-\Gamma_1-\Gamma_w \tag{2.4}$$

Momentum Equation:

$$\frac{\partial\left(\alpha_{fr}\rho_g v_g\right)}{\partial t}+\alpha_{fr}\rho_g v_g\nabla v_g=-\alpha_{fr}\nabla p-\alpha_{fr}\rho_g g-F_1-F_{wg} \tag{2.5}$$

$$\frac{\partial\left(\left(1-\alpha_{fr}\right)\rho_l v_l\right)}{\partial t}+\left(1-\alpha_{fr}\right)\rho_l v_l \nabla v_l = -\alpha_{fr}\nabla p-\left(1-\alpha_{fr}\right)\rho_l g - F_1 - F_{wf} \qquad (2.6)$$

Energy Equation:

$$\left(\frac{\partial\left(\alpha_{fr}\rho_g h_g\right)}{\partial t}\right)+\nabla\left(\alpha_{fr}\rho_g v_g h_g\right)=Q+E_1+E_w \qquad (2.7)$$

$$\left(\frac{\partial\left(\left(1-\alpha_{fr}\right)\rho_l h_l\right)}{\partial t}\right)+\nabla\left(\left(1-\alpha_{fr}\right)\rho_l v_l h_l\right)=Q-E_1-E_w \qquad (2.8)$$

As it can be understood these equations can be reduced to one dimensional system and usually it is the case in many of the reliable software codes; such as EUREKA and PARET. Besides, they may be reduced from six into three equations, if the flow is considered to be a single phase flow. The reduced form of the governing equations will be presented in Section 3.3.2.

The generic forms of the transient heat conductivity equations of a multi-dimensional system can be described as following;

$$k\nabla^2 T + q''' = \rho C_P \frac{\partial T}{\partial t} \qquad (2.9)$$

It is worth to mention that when it comes to reactor core, the thermal-hydraulic behavior depends on the assemblies and its fuel elements geometry, which can differ from rectangular, cylindrical, spherical or may even have more complicated shape such as the wire-wrapped assemblies. Therefore, it is really important to understand the geometrical range in which the proposed scheme and thermal-hydraulic correlations are valid. Finally, what drives the reactor to behave in a transient manner is represented by reactivity; which is a summation of external reactivity and reactivity feedbacks. Whereas the latter consists of reactivity feedbacks due to fuel temperature changes, moderator or coolant temperature changes and void presence. Hence, the reactivity $\rho(t)$ shown in Eq. 2.1 can be defined as following;

$$\rho(t) = \rho_{ext} + \Delta\rho_{Fuel} + \Delta\rho_{Moderator} + \Delta\rho_{Coolant} + \Delta\rho_{reflector} + \Delta\rho_{Void} \qquad (2.10)$$

2.2 Severe Accidents

The severity of the accidents categories is scaled by the amount and the degree of fuel damage. In better words, the severe accident occurs when the cladding barrier of the fuel rod is degraded and penetrated, causing a release of radioactive fission products to the surrounding environment. Thus, the integrity of the fuel element must be resilient and intact through any possible scenario, besides the operational one.

The most common analyzed severe accident scenarios are the following:

A. Loss of Coolant Accident (LOCA): It can be understood from its name that LOCA is an event where reactor coolant is lost, due to very small breaks of the reactor coolant system boundary to a double ended failure (rupture) in the largest pipe of primary circuit coolant. Hence, the primary coolant flow rate may rapidly degrade and depressurize. Therefore, the classification of LOCA can be related to the size of leak (i.e. Small, Medium, Large Break LOCA).

B. Loss of Flow Accident (LOFA): Unlike LOCA there is no break or leak, however, loss of coolant flow occurs due to pumping power being lost (i.e. due to electrical power loss).

C. Reactivity Initiated Accident (RIA): This type of accident can be classified into three categories as addressed by Miraz et al. [43];

   I. Quasi-static transients; the reactivity insertion rates are slow, in a way the feedback reactivity and control system reactivity (if existed) has enough time to compensate the reactivity insertion rate.

   II. Super-delayed critical transients; the reactivity insertion rate is rapid enough to cause the total reactivity to significantly rise, however, not enough to reach prompt critical.

   III. Super-prompt critical transients; the magnitude of reactivity insertion rate is large enough (whether due the reactivity insertion is high, it is very rapid, or both), causing the total reactivity to overcome the prompt critical, in which the delayed terms became negligible and the reactor transient responses become dependent mainly on prompt terms.

3. METHODOLOGY

3.1 Neutronic Analysis

Previously, a neutronic model was developed by Türkmen et al., using MCNP and neutronic analysis for ITU TRIGA Mark II was conducted [44], which also was used in further studies, such as; burnup effect analysis presented in [45]. Since this model included many simplifications, more accurate new model was developed and introduced prior to this work. The study introduced two models for simulating the neutronic behavior of ITU TRIGA Mark II research reactor, these models were developed using Monte-Carlo codes; Serpent 2 [46] and MCNP-V [47]. Furthermore, the models were benchmarked against the experimental data for excess reactivity determination at first criticality state presented in [35]. The 3D-models had thoroughly considered and included; the concrete building, the water pool, the reflector including the cavity region, all beam ports, the 91 positions in the core related to fuel elements, graphite dummies, control rods and irradiation tubes (central thimble and pneumatic system). Figure 3.1 represents a cross sectional view of the given described neutronic models.

Both models showed good agreements with the experimental data (with MCNP slightly better performance), and proved to be reliable for further studies. Because of that, confidence was built in implementing the described neutronic models in the current research. The Monte-Carlo models have been utilized in calculating the required neutronic parameters in solving the point kinetics equations and the reactivity feedback terms, which are presented in Table 3.1 and Table 3.2, respectively. In Table 3.1 two sets of data are presented when it comes to decay constant and delayed neutron fractions, the reason behind that is to check if the point kinetics solution (proposed in Section 3.3.1) fails. Besides, in order to investigate their influence on the concerned model. The neutronic flux distributions were extracted in a separate study, based on the mentioned Monte-Carlo models, and utilized to extract the power fraction distributions given in Appendix A.

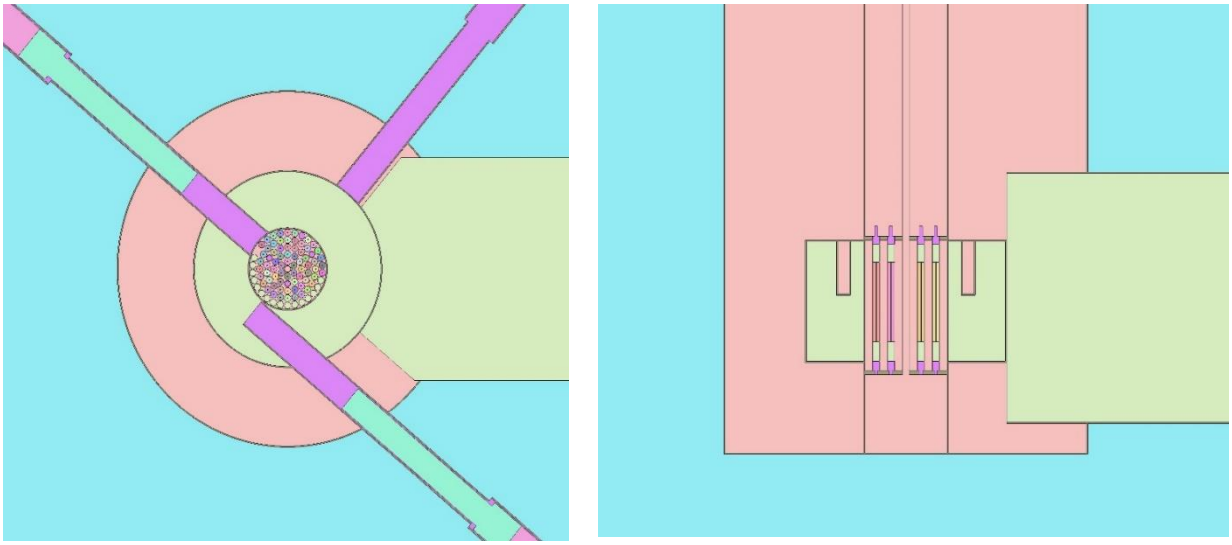

Figure 3.1 : Cross-sectional views radial (left) and axial (right) of the neutronic model for fresh fuel configuration.

Table 3.1 : Neutronic parameters of ITU TRIGA Mark II extracted using Serpent-2 model.

(i)	β_i	λ_i	β_i	λ_i	Λ (s)	β_{eff}
1	0.00025474	0.0124667	0.000262168	0.0133379		
2	0.00109069	0.0282917	0.00138021	0.032731		
3	0.00068041	0.0425244	0.00130354	0.1208		
4	0.0014448	0.133042	0.0029134	0.302934	5.3032E-5	0.00748
5	0.00241317	0.292467	0.00120081	0.850235		
6	0.00066634	0.666488	0.00048702	2.85584		
7	0.00060435	1.63478				
8	0.00016972	3.5546				

Table 3.2 : Fuel, coolant temperatures, and void presence effects on criticality.

Fuel Temperature Effect		Water Temperature Effect		Void Presence Effect	
Temperature (°C)	dk/k	Temperature (°C)	dk/k	Temperature (°C)	dk/k
27	0	27	0	0	0
51	-0.00069897	51	-0.00199	-0.15	-0.006126
70	-0.00349484	77	-0.00483	-0.25	-0.013407
90	-0.00563058	101	-0.00742	-0.5	-0.042337
127	-0.00916425	127	-0.00987		
161	-0.01510548				
327	-0.02989059				

3.2 EUREKA

EUREKA is a computer code for analyzing neutronic and thermal-hydraulic transient behaviors prior, during and post to reactivity accident scenarios, which means the analyses take place in a transient response of the reactor due to changes in fuel, moderator temperatures and coolant thermal-hydraulic behavior. EUREKA-2/RR is a revised version of the original EUREKA-2 code, developed in order to perform the mentioned analyses on research reactors. In this version, special CHF and heat transfer correlations have been implemented, which are applicable for research reactors. Moreover, the code can deal with both rectangular plate and cylindrical fuel elements. Besides, power level control system is added for transient simulation of a continuous automatic control system. The thermal-hydraulic system to be modelled is defined by interconnecting volumes (defined by the user), where only the fuel (heat generation) regions, bottom and upper plenums to be considered in the lumping scheme. Which means the system must be divided into number of regions (channels) with the corresponding coolant nodes and heat slabs (heat conductors).

EUREKA-2/RR considers the operating fluid in each control volume to be a one-dimensional homogenous fluid. The code solves both energy and continuity equations with respect to each node, while the momentum equation is solved at the lower and upper junctions of the concerned node. The correlations related to heat transfer differs in accordance to the direction and Reynolds number of the flow, therefore, the ones which concern the current research are mentioned here. The Sudo-Kaminage correlation is applied to calculate CHF, whereas the heat transfer coefficient for single phase calculated by Dittus-Boelter correlation. For two-phases fluid by Chen and Rosenow correlations, whereas the ONB state is determined by comparing the heat fluxes evaluated by applying the Dittus-Boelter and modified Chen correlations. One of the main limitations in EUREKA is that the point kinetics solution can only be solved by one set of decay constants and delayed neutron fractions, which are proposed by Chao and Attard [48]. The influence of not having the accurate set of neutronic parameters that is unique to each reactor is investigated and discussed more in Section 4. The code utilizes feedback reactivity weights at each control volume in order to calculate the summation of reactivity feedbacks emerged by all control volumes. One of the critical drawbacks in this code is the initialization for the transient solution, and

it is recommended to analyze the initial fields with caution before advancing in the analyses.

It can be referred to the manual [6] for better understanding on the methodology adapted in solving the necessary equations and linking them, which correlations, how to develop the input and reading the data from the output, and for any further information that might be needed concerning EUREKA-2/RR code.

In the current analysis, the thermal hydraulic system consists of 5 channels including 10 nodes and 10 heat slabs (which are the maximum possible numbers), while the number of junctions in one channel is 11. In addition, two plenums' volumes which make them in total 52 nodes and 56 junctions. The system as described is shown in Figure 3.2.

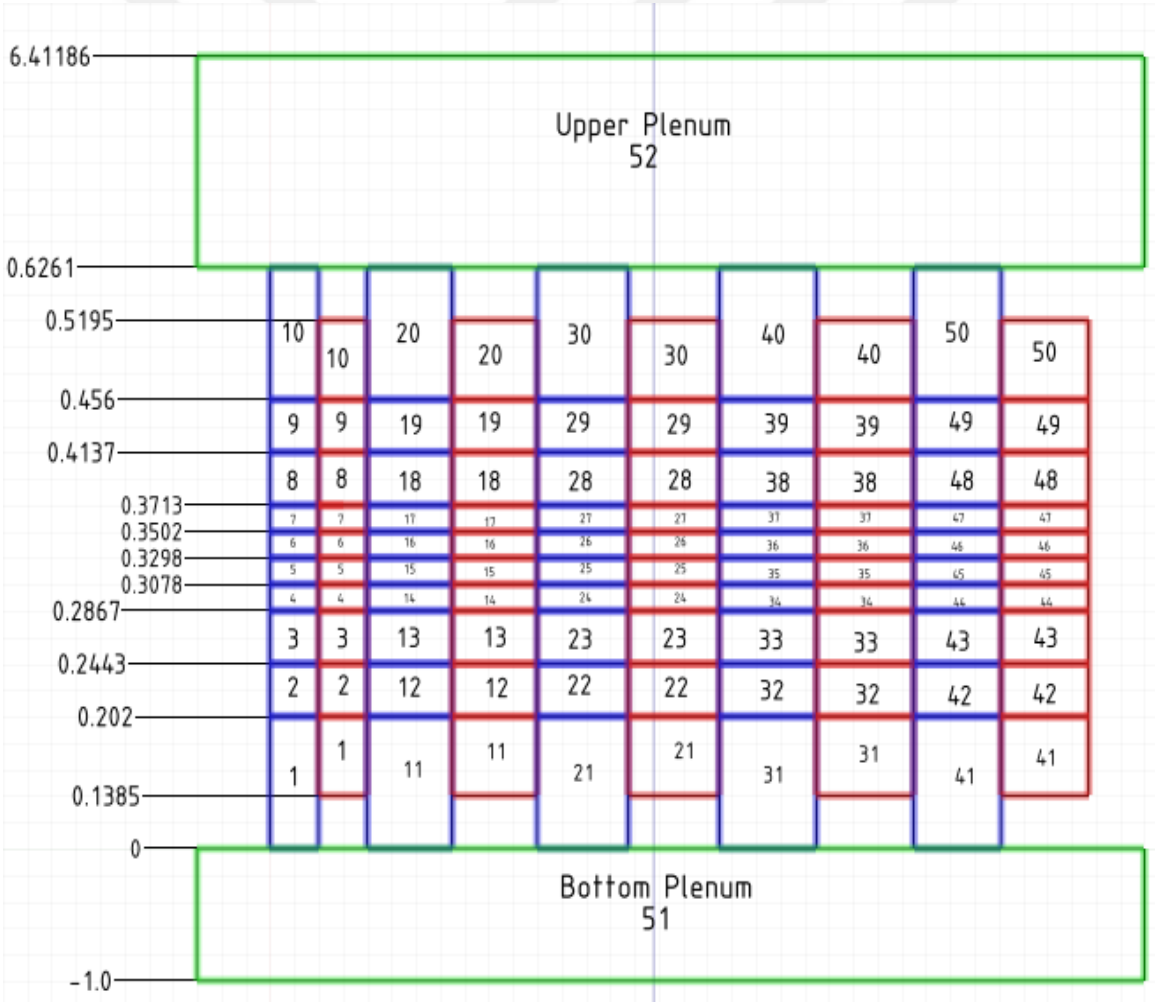

Figure 3.2 : Representation model of the EUREKA-2/RR analysis model, the axial coordinates on the left of the model represents the values in meter.

There are three associate codes with EUREKA code, which are; DISSUE calculates the power fraction distribution and the reactivity feedback weight of each heat slab segment, depending on the neutronic fluxes extracted by the neutronic code (in this case MCNP-V or Serpent 2). ICETEA calculates the initial temperature data for each node depending on the output of DISSUE. PREDISCO calculates the pressure distribution in each node based on the output of ICETEA. The effective delayed neutron fraction and prompt neutron generation lifetime presented in Table 3.1 and Table 3.2 have been utilized in the EURKEA-2/RR. Figure 3.3 gives a better insight on the relationships series of the codes in building the input data required for EUREKA-2/RR.

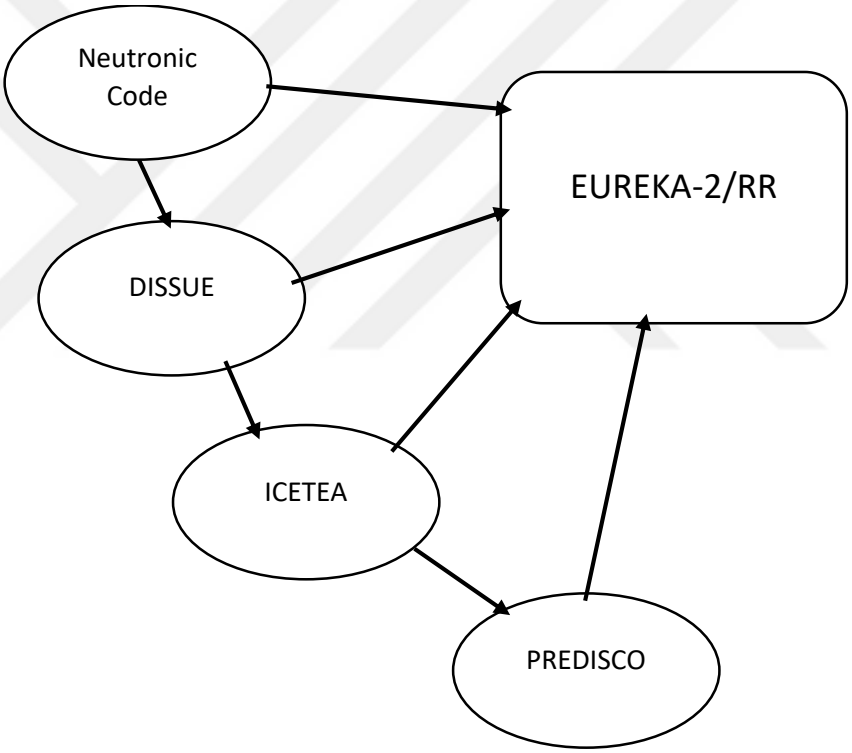

Figure 3.3 : Schematic representation in EUREKA-2/RR model input.

The power fraction distribution is provided in Appendix A (Table A.1), and Table 3.3 shows the difference in defining some of the hydraulic parameters, channel 1 is the hot channel which represents fuel element B-2 and the surrounding coolant channel. This channel is the critical channel in which fuel, cladding temperatures and DNBR (or CHF) may reach its critical values.

Table 3.3 : Hydraulic characteristic of each channel.

Channel #	Elements in channel	Area (m^2)	Mass Rate (Ton/hour)
1	1	0.000539	5.5372
2	15	0.008085	83.058
3	17	0.009163	94.133
4	20	0.01078	110.745
5	16	0.008624	88.596

It is worth to mention that since the neutronic analysis had been performed by Monte-Carlo codes using continuous energy cross-section libraries, it wasn't possible to determine accurate feedback reactivity weight at each volume (segment). That's due to the complexity in determining the adjoint fluxes using non-deterministic codes, giving away the continuous energy libraries that are used, which imposes another challenge in determining these fluxes. This issue had been addressed in different studies in the literature, such as; [49] and [50], where in both they have introduced iterated fission probability as a solution method for the addressed issue. Because of that two different sets of available data for different research reactors (TRR-1 [51] and JRR-3M [19]) have been tested and no significant difference have been resulted. Hence, the TRR-1 set of reactivity feedback weights data have been used for the current analysis, since TRR-1 has more in common with ITU TRIGA Mark II. Initially ten study cases of reactivity initiated accident scenarios were analyzed as following;

I. Reactivity insertion of $(\mathrm{dk/k})/\mathrm{step}=0.014/\mathrm{step}$ ($1.872\ \$/step$), step size = 0.01 second, unprotected.
II. Ramp reactivity, reactivity insertion of $(dk/k)/time = 0.014/time$ ($1.872\ \$/time$), step size = 0.5 second, unprotected.
III. Reactivity insertion of $(dk/k)/step = 0.014/step$ ($1.872\ \$/step$), step size = 0.01 second, scram at power level 2 MW with delay time = 0.1 second (slow scram).
IV. Reactivity insertion of $(dk/k)/step = 0.014/step$ ($1.872\ \$/step$), step size = 0.01 second, scram at power level 2 MW with delay time = 0.01 second (fast scram).
V. Reactivity insertion of $(dk/k)/step = 0.007/step$ ($0.935\ \$/step$), step size = 0.01 second, unprotected.

VI. Reactivity insertion of $(dk/k)/step = 0.007/step$ (0.935 $\$/step$), step size = 0.001 second, unprotected.

VII. Reactivity insertion of $(dk/k)/step = 0.007/step$ (0.935 $\$/step$), step size = 0.01 second, scram at power level 2 MW with delay time = 0.1 second.

VIII. Reactivity insertion of $(dk/k)/step = 0.0035/step$ ($0.468\$/step$), step size = 0.01 second, unprotected.

IX. Reactivity insertion of $(dk/k)/step = 0.0035/step$ ($0.468\$/step$), step size = 0.001 second, unprotected.

X. Reactivity insertion of $(dk/k)/step = 0.0035/step$ ($0.468\$/step$), step size = 0.01 second, scram at power level 2 MW with delay time = 0.1 second.

However, there was no significant observations between case VIII, IX and X, therefore, only case VIII is introduced in this research. Similarly, cases VI and V showed no obvious differences, hence, case V is only introduced. Which means total number of highlighted cases in this study is 7.

3.3 TM2-RIA Code Development

The code TM2-RIA (TRIGA MARK II Reactivity Initiated Accident code) is structured around a scriptable object-oriented framework using the programming language MATLAB. The code analyzes both steady-state and transient behavior of TRIGA Mark II reactor for a 2-dimensional (axial and radial) thermal hydraulic system, also simulates RIA scenarios for safety analysis. In this code the lumping thermal-hydraulic parameters technique [22] is adapted for the thermal hydraulic part, by dividing the system into two channels; hot and average channels with each channel including 18 even control volumes (segments). The code can be modified to consider different number of channels and control volumes. The power fraction distribution for operational power is shown in Table A.2 provided in Appendix A. The neutronic behavior is solved by considering the reactor as one point which allow the code to adapt a simple solution for the point kinetics when it comes to the power behavior with response to reactivity transient changes. Unlike EUREKA-2/RR, the point kinetics solution meant to give the chance to implement any neutronic precursors group data, corresponding to the analyzed reactor. The algorithm diagram of how this code operates is introduced in Figure 3.4.

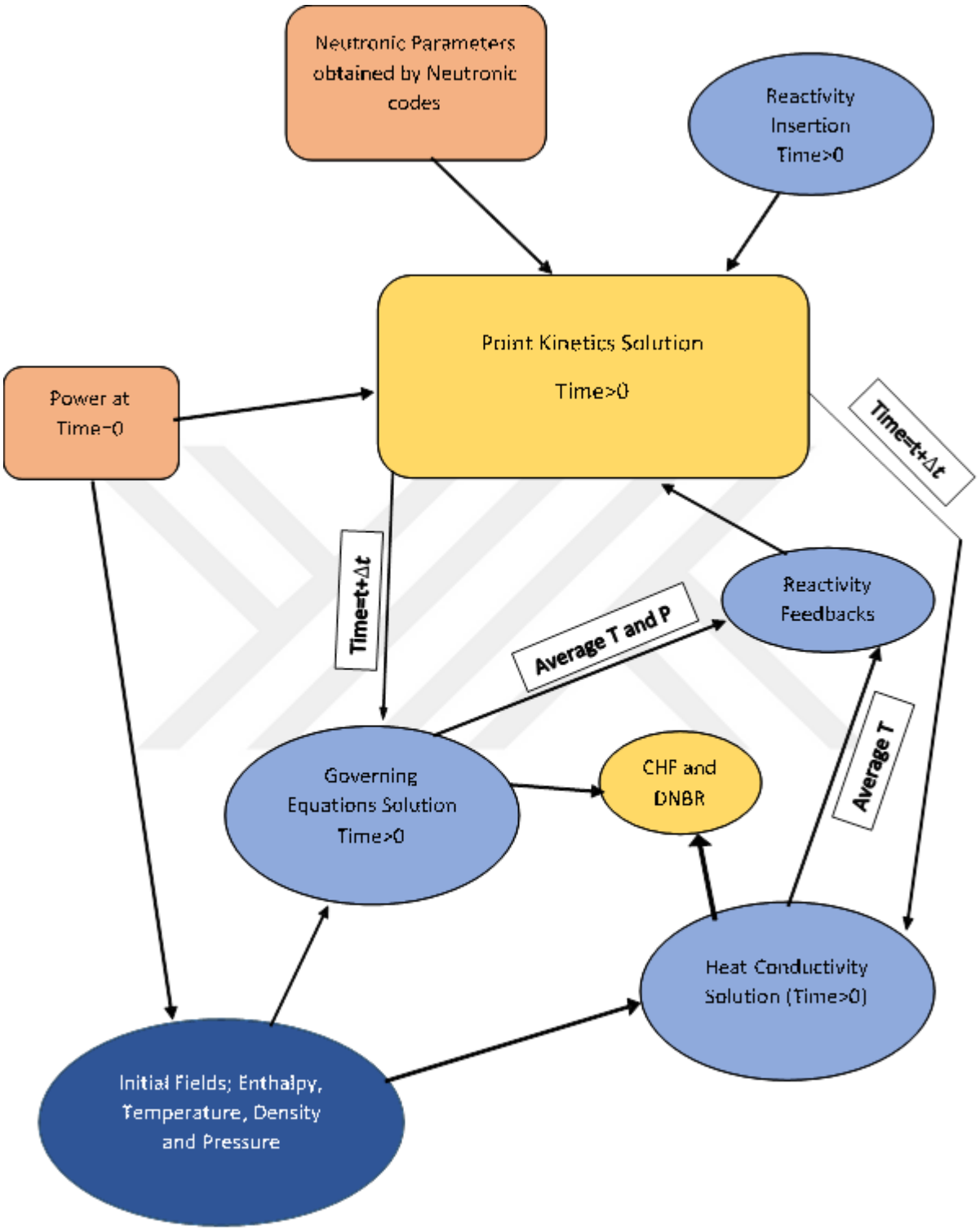

Figure 3.4 : Algorithm diagram of TM2-RIA.

3.3.1 Point kinetics equations

By recalling the point kinetics equations Eq. 2.1 and Eq. 2.2;

$$\frac{dn(t)}{dt} = \frac{\rho(t) - \beta_{eff}}{\Lambda} n(t) + \sum_{i=1}^{g} \lambda_i C_i(t) + S(t) \tag{3.1}$$

$$\frac{dC_i(t)}{dt} = \frac{\beta_i}{\Lambda} n(t) - \lambda_i C_i(t) \tag{3.2}$$

Where $i = 1, 2, \ldots, g$ represents precursors group number.

The Piecewise Constant function mentioned previously and presented in [41] has been adapted for the solution of point kinetics equations for TMII-RIA code, the solution starts by rewriting the equations in the following form:

$$\frac{d\vec{x}}{dt} = A\vec{x}(t) + B\vec{x}(t) + S(t) \tag{3.3}$$

Where $\vec{x}(t) = \left(n(t)\ \mathrm{C}_1(t)\ \ldots\ \mathrm{C}_g(t)\right)^T$

A and B are a $(g+1)x(g+1)$ matrices described as following;

$$A = \begin{pmatrix} -\frac{\beta_{eff}}{\Lambda} & \lambda_1 & \cdots & \lambda_g \\ \frac{\beta_1}{\Lambda} & -\lambda_1 & 0 & 0 \\ \vdots & 0 & \ddots & 0 \\ \frac{\beta_g}{\Lambda} & 0 & 0 & -\lambda_g \end{pmatrix} \quad \& \quad B = \begin{pmatrix} \frac{\rho(t)}{\Lambda} & 0 & \cdots & 0 \\ 0 & 0 & 0 & 0 \\ \vdots & 0 & \ddots & 0 \\ 0 & 0 & 0 & 0 \end{pmatrix} \tag{3.4}$$

While $\vec{S}(t)$ is a $(g+1)$ vector, defined as following;

$$\vec{S}(t) = \left(S(t)\ 0\ \ldots\ 0\right)^T \tag{3.5}$$

After multiplying both sides of Eq. 3.3 with the integral factor $e^{-(A+B_i)t}$, then by processing and evaluating the integration, the equation can be represented as following;

$$\vec{x}(t+\Delta t) = \vec{x}(t)e^{-(A+B_i)\Delta t} + (e^{-(A+B_i)\Delta t} - I)(A+B_i)^{-1}\vec{S}_i \qquad (3.6)$$

Where $\Delta t = t_{i+1} - t_i$

Eq. 3.6 can finally be represented as;

$$\vec{x}(t+\Delta t) = X_i e^{-D_i \Delta t} X_i^{-1}\vec{x}_i + (X_i e^{-D_i \Delta t} X_i^{-1} - I) X_i D_i^{-1} X_i^{-1}\vec{S}_i \qquad (3.7)$$

X_i represents the eigenvectors of $(A+B_i)$, while the eigenvalues $\omega_1^{(i)} \cdots \omega_g^{(i)}$ and $D_i = diag\left[\omega_1^{(i)} \cdots \omega_g^{(i)}\right]$.

Since $n(t)$ can be replaced by power $P(t)$, therefore, initial conditions at time=0;

$$\vec{x}(0) = \left(P(0) \ \frac{\beta_1}{\lambda_1 \Lambda} P(0) \ \ldots \ \frac{\beta_g}{\lambda_g \Lambda} P(0) \right)^T \qquad (3.8)$$

3.3.2 Heat conductivity equation

The transient heat conductivity equation for a radial one-dimension system can be described as following;

$$\frac{1}{r}\frac{\partial}{\partial r}\left(kr \frac{\partial T}{\partial r} \right) + q''' = \rho C_p \frac{\partial T}{\partial t} \qquad (3.9)$$

To solve Eq. 3.9 numerically, fully implicit finite difference method explained by Anderson et al. [52], is implemented in this model. This method gives more flexibility in defining the temporal and spatial steps, since the method is stable. Considering the temporal step number represented by $n = 1, 2, \ldots . N$ and the time step size is Δt, whereas the radial step number represented by $i = 1, 2, \ldots \ m + 1$ and the step size is Δr. Keeping in mind that solution is also applied in the vertical (z) axis as well, where the axial step number is represented by j. That being said, the only change takes place in the z direction is due to source in a radial direction, which will be presented in the next equation. Therefore, only radial discretization is presented here, the solution can be written as;

$$a_i T_{i-1}^{n+1} + b_i T_i^{n+1} + c_i T_{i+1}^{n+1} = d_i T_i^n + s_i \tag{3.10}$$

Where a_i, b_i, c_i and d_i are coefficients dependent on the radial dimension except on the clad surface, where they become influenced by z dimension, however, s_{ij} (source) depends always on both axial (z) and radial (r) dimensions.

For $R = 0$, since the system is considered symmetric at the centerline, at $R = 0$ the system is adiabatic, which means $\frac{\partial T}{\partial r} = 0$. Therefore;

$$a_i = 0,\ \ b_i = \left(1 + \frac{\Delta \mathrm{R}_\mathrm{f}^2}{4\alpha_f \Delta t}\right),\ \ c_i = -1,\ d_i = \left(\frac{\Delta \mathrm{R}_\mathrm{f}^2}{4\alpha_f \Delta t}\right) T_{ij}^n + q_j'''^{n+1}\left(\frac{\Delta \mathrm{R}_\mathrm{f}^2}{4k_f}\right) \tag{3.11}$$

For $0 < R_i < R_f$ (fuel interior region);

$$a_i = R_i - \Delta R_f / 2,\ \ b_i = \left(2R_i + \frac{R_i \Delta \mathrm{R}_\mathrm{f}^2}{\alpha_f \Delta t}\right),\ \ c_i = R_i + \Delta R_f / 2,$$
$$d_i = \frac{R_i \Delta \mathrm{R}_\mathrm{f}^2}{\alpha_f \Delta t} T_{ij}^n + q_j'''^{n+1}\left(\frac{R_i \Delta \mathrm{R}_\mathrm{f}^2}{k_f}\right) \tag{3.12}$$

At fuel-clad interface surface $R_i = R_f$, here both clad and fuel play role in the heat conductivity equation;

$$a_i = -(R_i - \Delta R_f / 2),$$
$$b_i = \left(\frac{k_{cl}}{k_f}(R_i - \Delta R_{cl} / 2) + (R_i - \Delta R_f / 2) + \frac{R_i \Delta \mathrm{R}}{2\Delta t}\left(\frac{1}{\alpha_f} + \frac{k_{cl}}{k_f \alpha_{cl}}\right)\right),$$
$$c_i = -\frac{k_{cl}}{k_f}(R_i - \Delta R_{cl} / 2),\ d_i = \frac{R_i \Delta \mathrm{R}}{2\Delta t}\left(\frac{1}{\alpha_f} + \frac{k_{cl}}{k_f \alpha_{cl}}\right) T_{ij}^n + q_j'''^{n+1}\left(\frac{R_i \Delta \mathrm{R}}{2k_f}\right) \tag{3.13}$$

For $R_f < R_i < R_{cl}$ (clad interior region), where there is no heat generation term anymore;

$$a_i = R_i - \Delta R_{cl}/2,\ \ b_i = \left(2R_i + \frac{R_i \Delta \mathrm{R}_{\mathrm{cl}}^2}{\alpha_{cl}\Delta t}\right),$$
$$c_i = R_i + \Delta R_{cl}/2,\ d_i = \frac{R_i \Delta \mathrm{R}_{\mathrm{cl}}^2}{\alpha_{cl}\Delta t} T_{ij}^n \tag{3.14}$$

At clad outer surface $R_i = R_{cl}$, here both clad and coolant play role in the heat conductivity equation;

$$a_i = -(R_i - \Delta R_{cl}),\ \ b_i = \left(\frac{h_c}{k_{cl}}(R_i + \Delta R_{cl})\Delta R_{cl} + 1 + \frac{R_i \Delta \mathrm{R}_{\mathrm{cl}}^2}{\alpha_{cl}\Delta t}\right),\ \ c_i = 0,$$
$$d_i = \frac{R_i \Delta \mathrm{R}_{\mathrm{cl}}^2}{\alpha_{cl}\Delta t} T_{ij}^n + T_{bulk,j}^n \frac{h_c}{k_{cl}}(R_i + \Delta R_{cl})\Delta R_{cl} \tag{3.15}$$

By rewriting the solution in Eq. 3.10 as;

$$AT(t + \Delta t) = B(t) \tag{3.16}$$

Where the coefficient matrix is a tridiagonal matrix as presented below;

$$A = \begin{pmatrix} b_1 & c_1 & 0 & \cdots\cdots & 0 \\ a_2 & b_2 & c_2 & 0 \cdots & 0 \\ 0 & a_3 & b_3 & c_3 & 0 \cdots 0 \\ \vdots & & \ddots & \ddots & \ddots \\ \vdots & & & a_m & b_m \quad c_m \\ 0 & \cdots\cdots & 0 & a_{m+1} & b_{m+1} \end{pmatrix} \tag{3.17}$$

And the vectors: $T(t + \Delta t) = \left(T_1^{n+1}\ \ T_2^{n+1}\ \ \ldots\ T_{m+1}^{n+1}\right)^T$ and $B(t) = \left(B_{1j}^n\ \ B_{2j}^n\ \ \ldots\ B_{m+1,j}^n\right)^T$

For more details on how the coefficient matrix been derived, it can be referred to [28].

3.3.3 Governing equations

Continuity, momentum and energy equations for one dimensional transient flow in vertical direction are represented respectively as described in [26];

Continuity Equation:

$$\frac{\partial \rho}{\partial t} + \frac{\partial G}{\partial z} = 0 \tag{3.18}$$

Momentum Equation:

$$\frac{\partial G}{\partial t} + \frac{\partial}{\partial z}\left(\frac{\partial G^2}{\partial \rho}\right) = -\frac{\partial p}{\partial z} - \left(\frac{f}{\rho}\right)\left(\frac{G^2}{2D_e}\right) - \rho g \tag{3.19}$$

Energy Equation:

$$\rho\left(\frac{\partial h}{\partial t}\right) + G\left(\frac{\partial h}{\partial z}\right) = 2q'' / d \tag{3.20}$$

Note: both $\rho + G$ are for homogenous flow, but since the current model doesn't deal with two-phase fluid flows, they are both considered to be only for liquid phase.

These equations are solved in this model by applying a fully implicit finite difference scheme, considering the temporal step number represented by $n = 1, 2, \ldots . N$ and the axial step number is represented by $j = 1, 2, \ldots, k + 1$.

The numerical solutions of Eq. 3.18, Eq. 3.19 and Eq. 3.20 are shown respectively below:

Continuity Equation:

There is a negligible change in density with time change, therefore, the first term in the left side of Eq. 3.18 is taken as zero and the solution becomes;

$$v_i^{n+1} = v_{i-1}^{n+1}\left(\frac{\rho_{i-1}^{n+1}}{\rho_i^{n+1}}\right) \tag{3.21}$$

Momentum Equation:

$$p_i^{n+1} = p_{i-1}^{n+1} - \Delta z \frac{\rho_i^{n+1}\left(v_i^{n+1} - v_i^n\right)}{\Delta t} - \ldots \tag{3.22}$$
$$\rho_i^{n+1}\left(v_i^{n+1}\right)^2\left(\frac{1}{\rho_i^{n+1}} - \frac{1}{\rho_{i-1}^{n+1}}\right) - g\Delta z \rho_i^{n+1} - HL_i^{n+1}$$

Where; $HL_i^{n+1} = \frac{\Delta z f_i^{n+1}}{2D_h} \rho_i^{n+1} \left(v_i^{n+1} \right)^2$

Energy Equation:

$$(1 + G_i^{n+1} \frac{\Delta t}{\rho_i^{n+1} \Delta z}) h_i^{n+1} = h_i^n + \left(G_i^{n+1} \frac{\Delta t}{\rho_i^{n+1} \Delta z} \right) h_{i-1}^{n+1} + \frac{2q'' \Delta t}{\rho_i^{n+1} d} \quad (3.23)$$

3.3.4 Reactivity

As mentioned before, the linking between the reactor kinetics and thermal-hydraulics is defined by the variable reactivity $\rho(t)$, there have been different approaches in determining the reactivity feedbacks. A simple and a common approach is applied in TM2-RIA to perform the calculations of Eq. 2.10, one average value is taken for fuel temperature, coolant density, and temperature of the whole core at each time step. Whereas the initial temperatures and density are considered to be the reference values, hence, the reactivity feedback terms can be described as;

$$\Delta\rho_{fuel} = \alpha_{Doppler} \left(T_{av}(t) - T_{av}(0) \right)_{fuel} \quad (3.24)$$

$\alpha_{Doppler}$ Doppler feedback coefficient ($\frac{\$}{°C}$)

$$\Delta\rho_{coolant} = \alpha_{coolant} \left(T_{av}(t) - T_{av}(0) \right)_{coolant} \quad (3.25)$$

$\alpha_{Coolant}$ Coolant feedback coefficient ($\frac{\$}{°C}$)

$$\Delta\rho_{void} = \alpha_{Void} \left(Density_{av}(t) - Density_{av}(0) \right) \quad (3.26)$$

α_{Void} Void feedback coefficient ($\frac{\$}{kg/m^3}$)

3.3.5 Heat transfer and CHF correlations

Heat transfer correlations:

Subcooled liquid convection condition;

$\mathrm{Re} \leq 2200$

$$h_c = 4k_c / D_h \tag{3.27}$$

$\mathrm{Re} > 2500$

Dittus-Boelter's correlation;

$$h_c = \frac{k_c}{D_h}(0.023\mathrm{Re}^{0.8}\,\mathrm{Pr}^{0.4}) \tag{3.28}$$

$$q'' = h_c(T_{cl} - T_{bulk}) \tag{3.29}$$

Where $\mathrm{Re} = \rho D_h v / \mu$ and $\mathrm{Pr} = C_p \mu / k_c$

Subcooled boiling region, then the onset nucleate boiling temperature is calculated in order to calculate the nucleate boiling heat transfer coefficient, that is achieved in this model according to Bergles-Rohsenow correlation [53];

$$T_{ONB} - T_{SAT} = 0.556\left(\frac{q''_{ONB}}{1082p^{1.156}}\right)^{0.463p^{0.0234}} \tag{3.30}$$

$$q'' = h_{NB}(T_{cl} - T_{sat}) + h_c(T_{cl} - T_{bulk}) \tag{3.31}$$

$$h_{NB} = 0.0012\left[\frac{k_c^{0.79}C_{pc}^{0.45}\rho_l^{0.49}}{\sigma_c^{0.5}\mu_c^{0.29}h_{\mathrm{lg}}^{0.24}\rho_g^{0.24}}\right](T_{cl} - T_{sat})^{0.24}\left(p_{sat(T=cl)} - p_{sat(T=T_{sat})}\right)^{0.75}S \tag{3.32}$$

Whereas; $S = \dfrac{1}{1 + 2.53x10^{-6}\,\mathrm{Re}^{1.17}}$

The thermodynamic parameters for the heat transfer package is estimated by using the set of formulas presented in [27].

For CHF Sudo-Kaminage correlation [6], is applied;

$$q''_{DNB} = q_s\left(h_{\mathrm{lg}}\sqrt{\lambda\rho_g g\left(\rho_l - \rho_g\right)}\right) \tag{3.33}$$

Whereas;

$$\left[\begin{array}{l} \lambda = \sqrt{\dfrac{\sigma}{\left(\rho_l - \rho_g\right)}},\ q_{s1} = 0.005 G_s^{0.611},\ G_s = \dfrac{G}{\sqrt{\lambda \rho_g g\left(\rho_l - \rho_g\right)}} \\ q_{s2} = 0.7 \dfrac{A_{flow}}{A_{slab}} \dfrac{\sqrt{d/\lambda}}{\left(1+\left(\rho_g/\rho_l\right)^{0.25}\right)^2},\ q_s = \max(q_{s1}, q_{s2}) \end{array}\right] \tag{3.34}$$

Besides, all thermodynamic parameters needed in solving previous and the upcoming equations are determined using Table B.1 provided in Appendix B.

3.3.6 Initial fields and steady-state case

In order to initiate the solutions for transient mode, thermal heat conductivity from fuel centerline till coolant, enthalpy and pressure fields must be determined. Besides, these values correspond to the steady-state condition of the concerned system.

Heat conductivity equation, independent of time in fuel region;

$$\frac{1}{r}\frac{\partial}{\partial r}\left(kr\frac{\partial T}{\partial r}\right) + q''' = 0 \tag{3.35}$$

The analytical solution for heat conductivity equation is derived similar to what was presented Bergman et al. [54], by integrating twice with respect to (r), the temperature distribution in fuel region is described as;

$$T(r) = Tm - \frac{r^2}{4k_f} q''' \tag{3.36}$$

Where Tm represents the centerline temperature of the fuel element.

For cladding region:

$$\frac{1}{r}\frac{\partial}{\partial r}\left(kr\frac{\partial T}{\partial r}\right) = 0 \tag{3.37}$$

Considering that at the fuel surface $-k_{cl}\left.\dfrac{\partial T}{\partial r}\right|_{R_f} = q''$

Hence;

$$T(r) = T_{cl} + q'' \frac{R_f^2}{2k_{cl}} \ln\left(\frac{R_{cl}}{r}\right) \tag{3.38}$$

Clad-Coolant interface:

$$T(r) = T_b + \frac{q''}{h_c} \tag{3.39}$$

Fuel Centerline Temperature:

$$Tm = T_b + \Delta T_{fuel} + \Delta T_{clad} + \Delta T_{coolant} \tag{3.40}$$

Similar to the previous proposed model for transient mode, the heat generation differs with respect to z direction, hence, the heat conductivity solution for steady-state is applied for the spatial steps on z direction (k+1).

Coolant temperature profile in z direction can be found by taking energy equation and removing the transient term, in which it becomes as following;

$$\Delta h = P / \dot{m} \tag{3.41}$$

Where Δh is the enthalpy difference between two junctions in z direction of a volume segment. Hence, the temperature difference between two junctions

$$\Delta T = \Delta h / C_p \tag{3.42}$$

Keeping in mind that the inlet temperature is supposed to be constant throughout the analysis (for both Transient and Steady-state modes).

Pressure profile through z direction is found by solving reducing the momentum equation into Bernoulli equation, which described as following;

$$\frac{P_j}{\gamma_j} + \frac{V_j^2}{2g} + z_j = \frac{P_{j+1}}{\gamma_2} + \frac{V_{j+1}^2}{2g} + z_{j+1} - HL - HF \tag{3.43}$$

HL and HF are major and minor losses, respectively. Which are described by Munson et al. [55] as following;

$$HF = K_L \frac{V^2}{2g}, HL = \frac{\Delta z f}{2D_h} \rho(v)^2 \tag{3.44}$$

Assuming that the wall is smooth, then the friction factor is dependent on Reynolds number.

$$\mathrm{Re} = \rho D_h v / \mu \tag{3.45}$$

if $\mathrm{Re} \le 2200$ then;

$$f = 64 / \mathrm{Re} \tag{3.46}$$

if $2200 < \mathrm{Re} < 3000$ then according to [23];

$$f = \left(3.75 - \frac{8250}{\mathrm{Re}}\right)(f_{\mathrm{Re}=3000} - f_{\mathrm{Re}=2200}) + f_{\mathrm{Re}=2200} \tag{3.47}$$

While if $\mathrm{Re} \ge 3000$ then Blasius formula shown in [55];

$$f = 0.316\mathrm{Re}^{-0.25} \tag{3.48}$$

Also friction factor values can be calculated by Moody-Chart given in Appendix C. The formulas of loss coefficient due to sudden formation change in reactor are described by Todreas and Kazimi [56] as:

Sudden Expansion:

$$K_L = \left(1 - (\frac{A_{small}}{A_{large}})^2\right) \tag{3.49}$$

Sudden Contraction:

$$K_L = 0.45\left(1 - (\frac{A_{small}}{A_{large}})\right) \tag{3.50}$$

4. RESULTS AND DISCUSSION

4.1 Safety Analysis Using EUREKA-2/RR

As mentioned in previously in Section 3.2, out of 10 different cases that have been studied, only seven cases are presented in this section. Keeping in mind that for all cases, reactivity insertion and the point kinetics calculations starts at time=1 seconds. All the cases initiated at operational power 0.25 MW, and the results presented in this section are for the hot channel.

Figure 4.1 till Figure 4.5 show the reactor transient behavior due to its response caused by the reactivity insertions influence (the study cases are V, VII and VIII as addressed in section 3.2)

Figure 4.1 shows how power levels increase rapidly to almost the same peak level) around 3 MW) in both cases for reactivity insertion=0.007/step (protected and unprotected), where it happened to take place almost at the same time location. However, the behavior afterwards changes significantly due to the total reactivity responses at each time step as shown in Figure 4.2. In the unprotected case; the reactor's power drops gradually till almost 1 MW, while the drop in power is much faster in the protected case. The reason behind that is the influence of the automatic control system that takes place when the reactor's power reaches 2 MW, which drops the total reactivity rapidly to negative values. It means that reactivity insertion is overwhelmed by the total negative reactivity feedbacks, causing the reactor's power to drop even lower than its operational power. On the other hand, in case of reactivity insertion=0.0035/step; there is no rapid and strong peak in power level, the power reaches its peak much slower, then the reactor's power takes a much steadier shape in a shorter time than the other two cases. Therefore, the RIA incident of 0.0035/step (step=0.01 sec) in case of ITU TRIGA Mark II, can be considered as Quasti-Static transient after reaching its peak power.

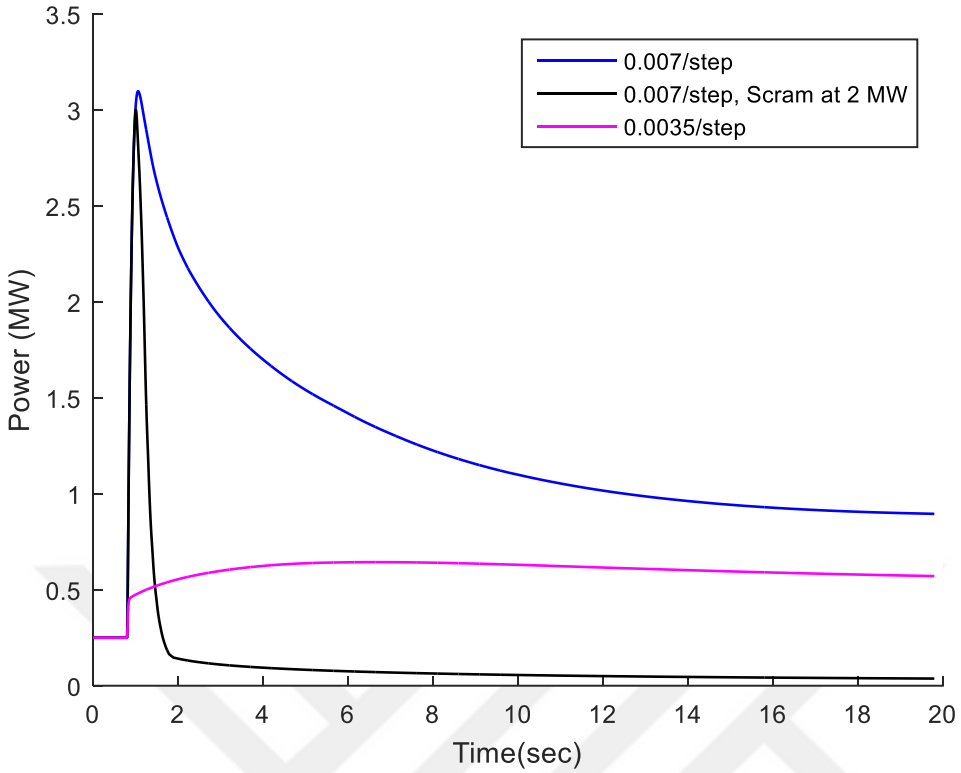

Figure 4.1 : Power vs time.

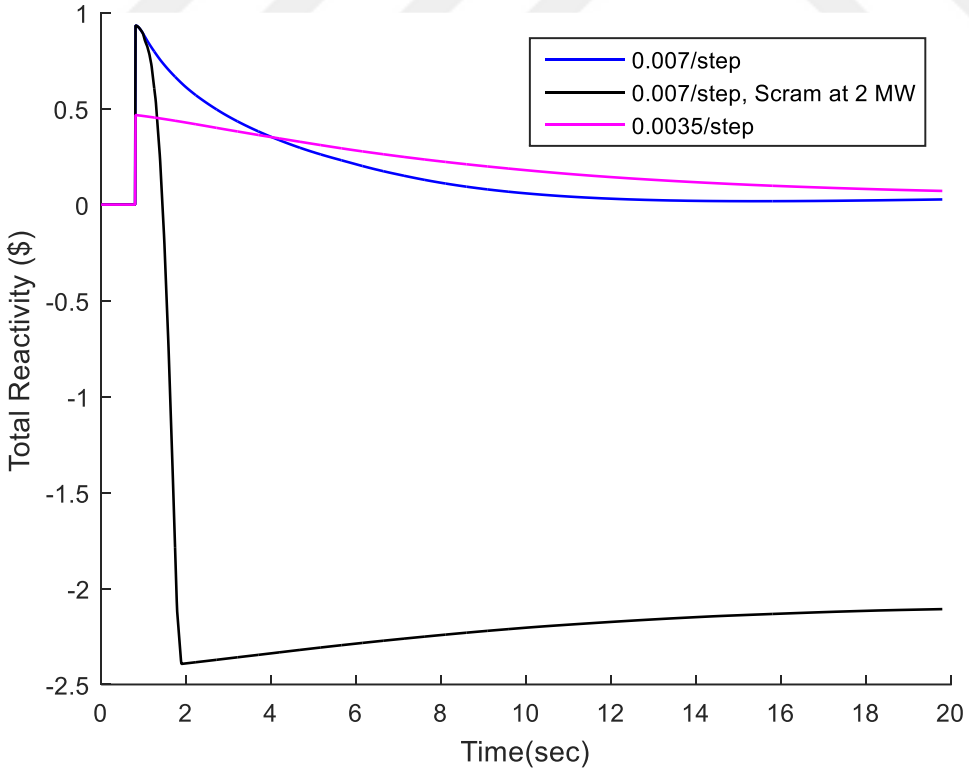

Figure 4.2 : Total reactivity change vs time.

The behavior of fuel temperature gives a better picture how reactivity feedbacks is changing. As it was concluded by the analysis in [1], for a cold startup the reactor reactivity feedbacks are mainly dominant by the Doppler broadening effect due to the change in fuel temperature. Indeed, the behaviors of average fuel temperature changes shown in Figure 4.3 reflects the behavior of total reactivity changes. In fact, the time steps at which fuel temperature peak, turning point and the almost steady behavior take place exactly at the same time intervals with respect to the trends of the total reactivity changes.

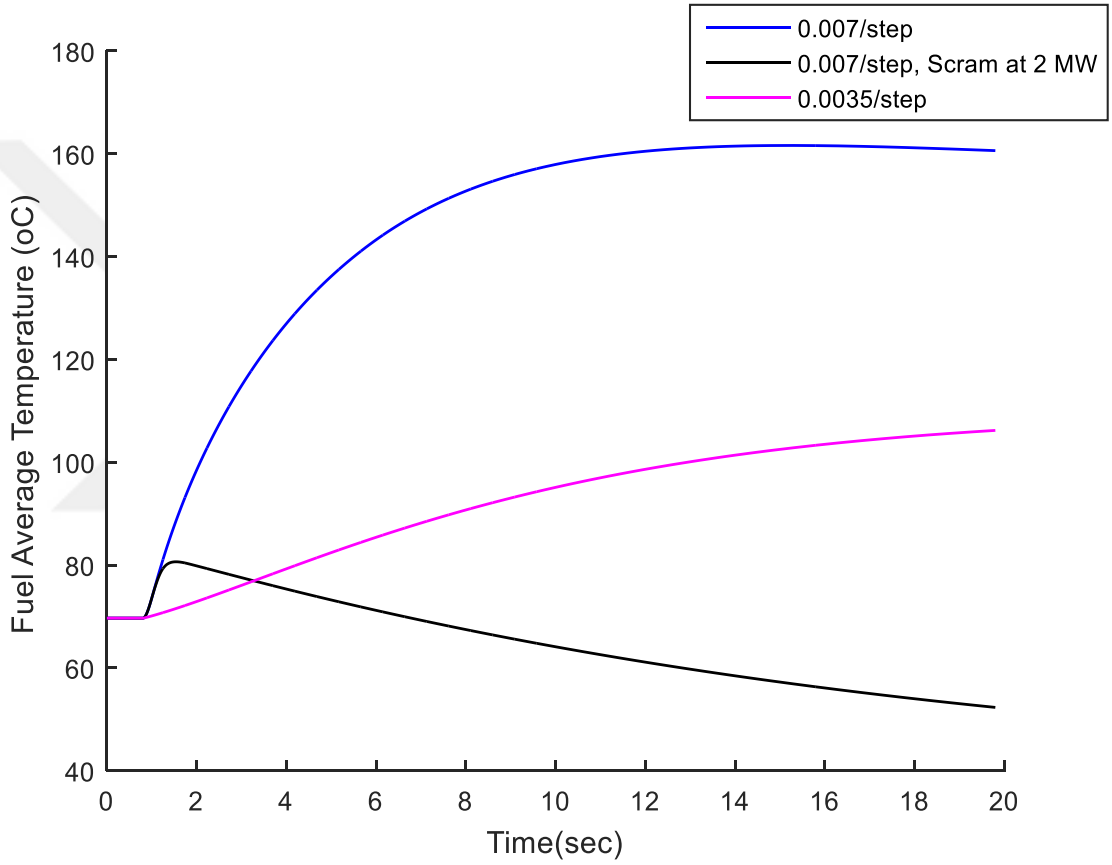

Figure 4.3 : Fuel average temperature vs time at the hottest segment.

The exact behavior is observed in cladding temperature transient behaviors shown in Figure 4.4 compare to the trends shown in Figure 4.3. But as expected the temperatures drop to lower magnitudes, since fuel region is a heat source, whereas, the heat reaches the cladding surface through conductivity of the fuel and cladding materials. Besides, the influence of the reactivity insertion rate's magnitude and the presence of automatic scram is very obvious in Figure 4.3 and Figure 4.4. Therefore, extracting such results

is very crucial to understand the non-linear transient behavior of a reactor during RIA events.

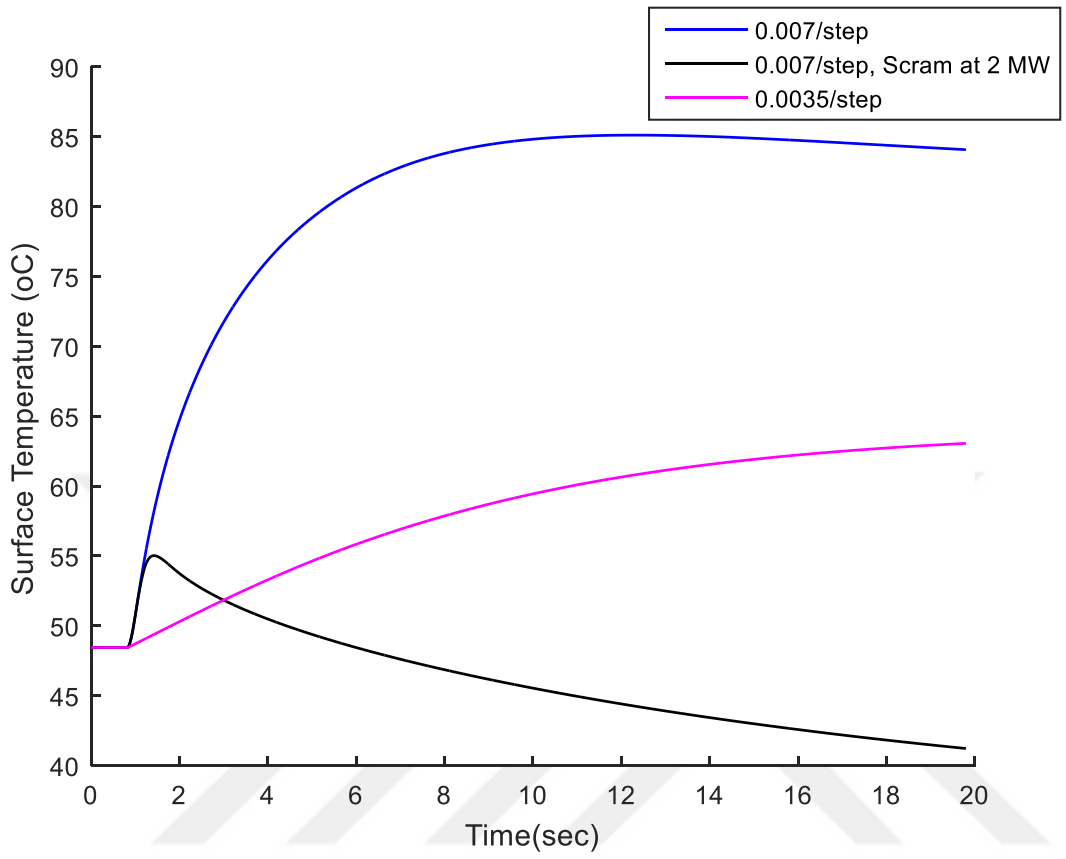

Figure 4.4 : Cladding surface temperature vs time at the hottest segment.

In addition, the cladding surface temperature transient change is related to the DNBR change trend shown in Figure 4.5. It can be concluded from this figure that DNBR drops not significantly and takes a steady shape in case of 0.0035/step rapidly. This corresponds to the trend shown in Figure 4.4.

On the contrary, DNBR drops for a much lower magnitude in case of 0.007/step, then starts increasing linearly but slowly in the unprotected case. On the other hand, for the protected case drops to its minimum value, which is almost two times bigger than what is predicted in the protected case. After that the DNBR increases much faster but also in almost linear behavior, reaching values higher than the operational case in a very short time, which reflects the strong negative reactivity feedbacks influence.

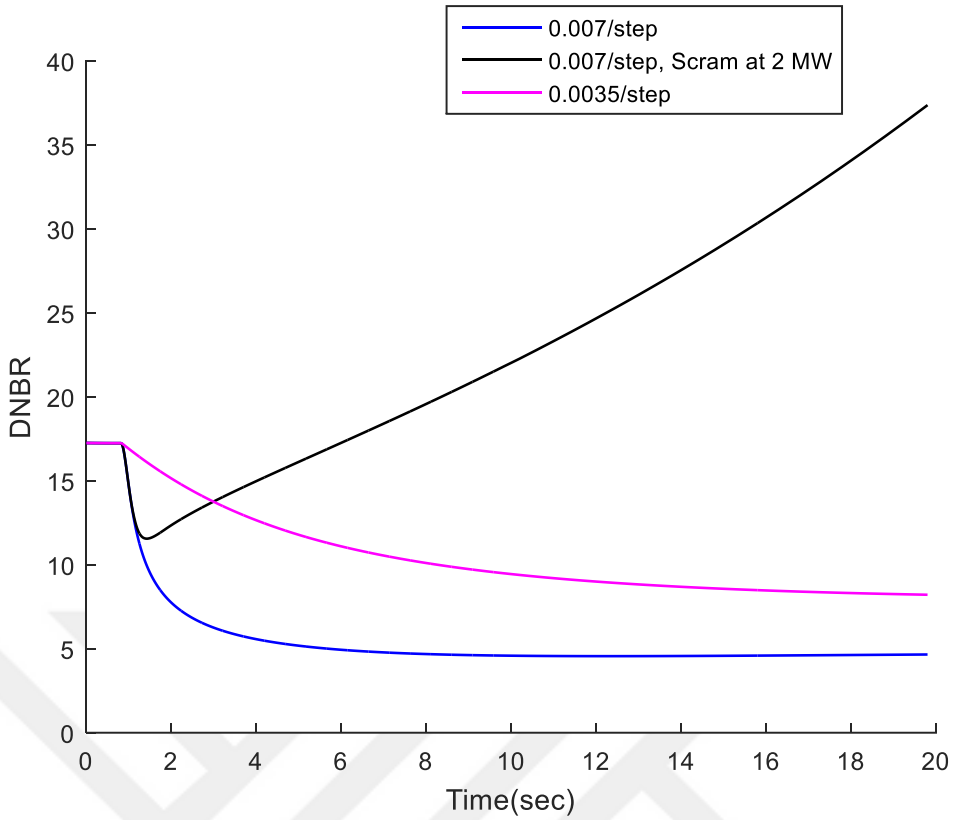

Figure 4.5 : DNBR change vs time at the hottest segment.

Figure 4.6 till Figure 4.11 represent the results of the addressed study cases (I-IV) in section 3.2, many aspects related to the relationships of power, total reactivity, presence of automatic scram, Doppler broadening, fuel temperature, cladding temperature, and DNBR transient behaviors. They are similar to what have been presented and discussed in the previous set of results. However, the currently investigated results gives insight on the influence of reactor's time response at a high level reactivity insertion rate of 1.872$/time. It can be seen from Figure 4.6, that when external reactivity is inserted at every time step (0.01 sec), the power reaches a very high level (above 450 MW), and the behaviors almost matched for both protected and unprotected cases, also no significant difference can be seen when the scramming control system reacts faster (~15 Megawatts below). On the other hand, there is a shift in time (clearly shown in Figure 4.7) around 0.35 seconds, when the external reactivity is inserted once every 0.5 seconds. The peak power in case of slow RIA event, reaches a magnitude of (~120 MW), which is much lower than the fast RIA event. The reason behind that, can be seen in Figure 4.8, the maximum total reactivity reaches a lower level than that in the other 3 cases, because the reactivity is being fed back at every step while the external feedback is playing role only once every 0.5 seconds, unlike

the other cases where the external reactivity is inserted every time step. Despite that, both the unprotected cases match after almost 15 seconds, because the reactor transient reached a Quasi-static state, where both external and reactivity feedback reach almost equilibrium.

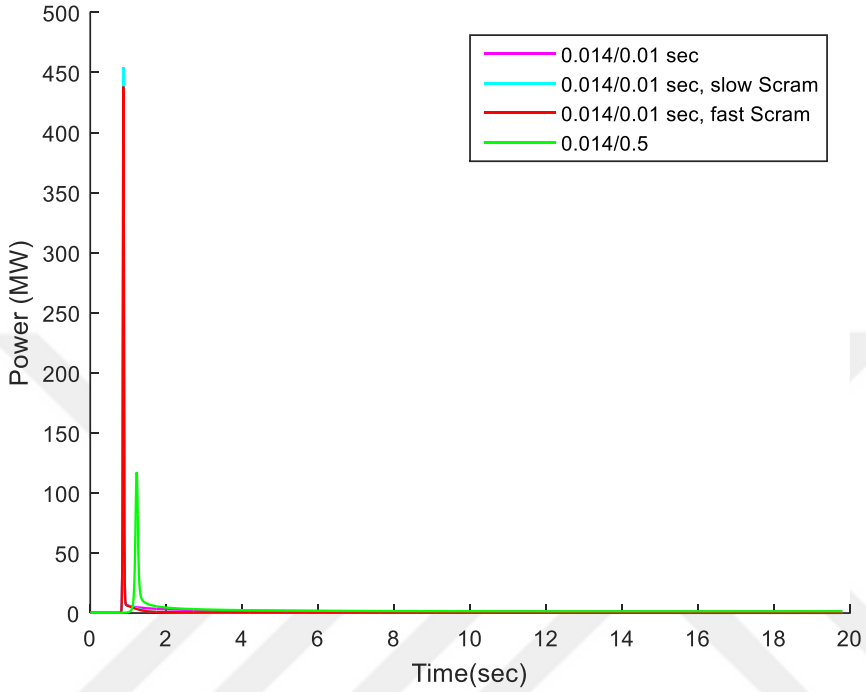

Figure 4.6 : Power vs time.

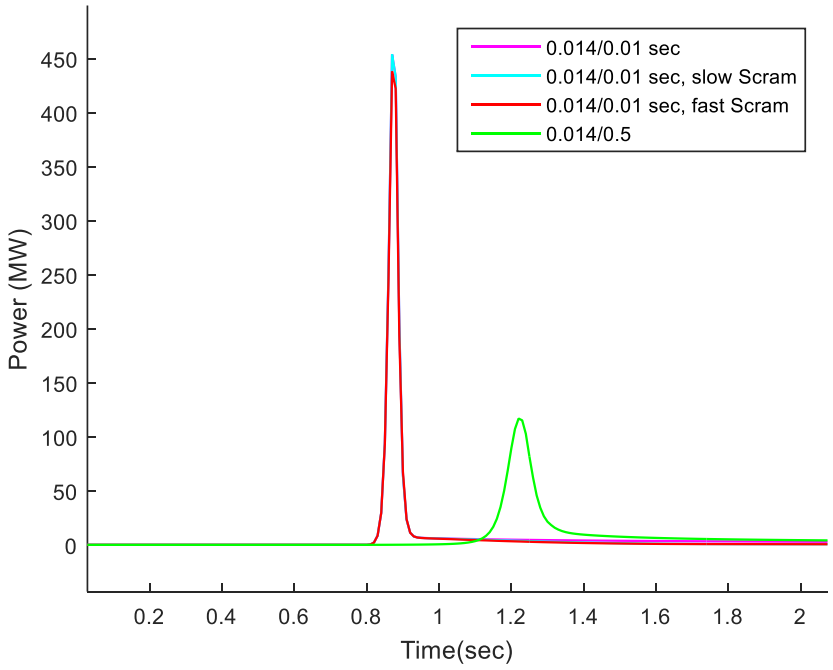

Figure 4.7 : Power vs time.

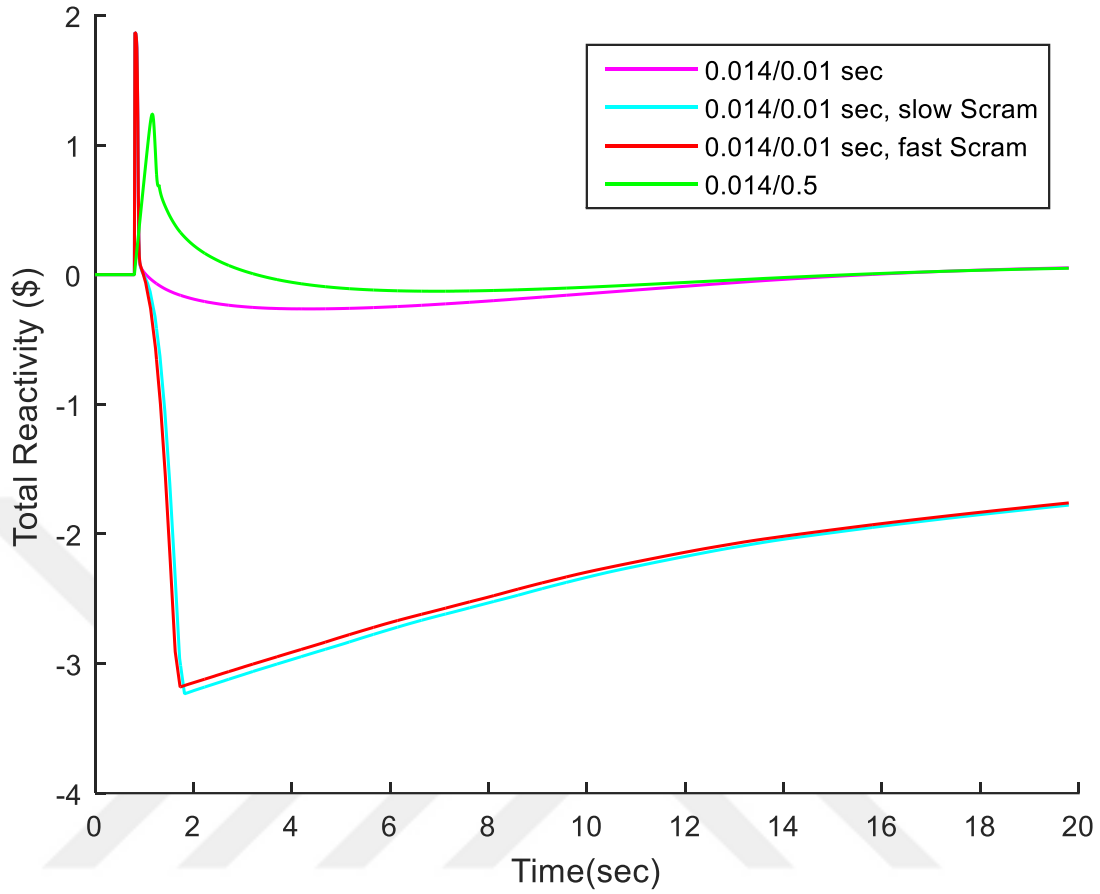

Figure 4.8 : Total reactivity change vs time.

That being said, the influence of automatic control is more pronounced in Figure 4.9 till Figure 4.11, the protection element has a strong impact in dropping the fuel and cladding surface temperatures, leading to an increase in the DNBR values. On the other hand, in case of ramp reactivity insertion the reactor responses in a similar trend to the step reactivity insertion, however, in a slower and in a less significance. But it doesn't cause a strong decline in total reactivity. In fact, more interestingly the total reactivity in case of unprotected step reactivity insertion, it reaches lower magnitude than ramp reactivity insertion as shown in Figure 4.8. It can be related to the impact of the strong negative Doppler reactivity coefficient feature in ITU TRIGA Mark II, caused by the temperatures reaching higher magnitudes in comparison to the other event, which induces a stronger reactivity feedback, as shown in Figure 4.9.

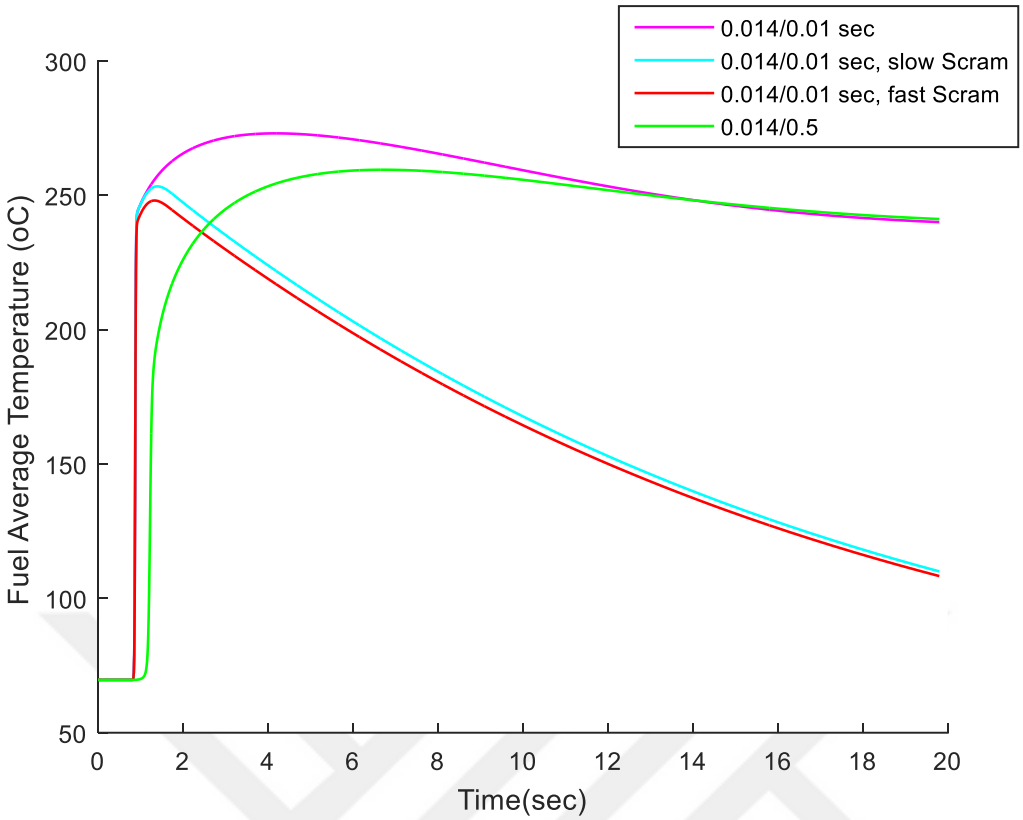

Figure 4.9 : Fuel average temperature vs time at the hottest segment.

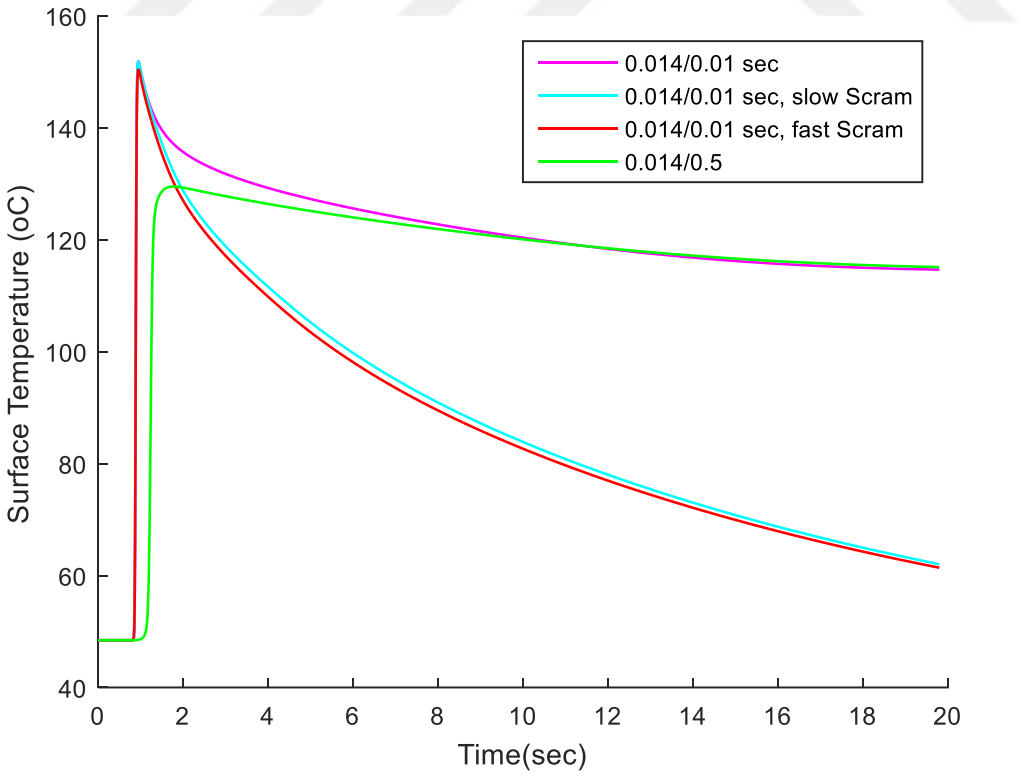

Figure 4.10 : Cladding surface temperature vs time at the hottest segment.

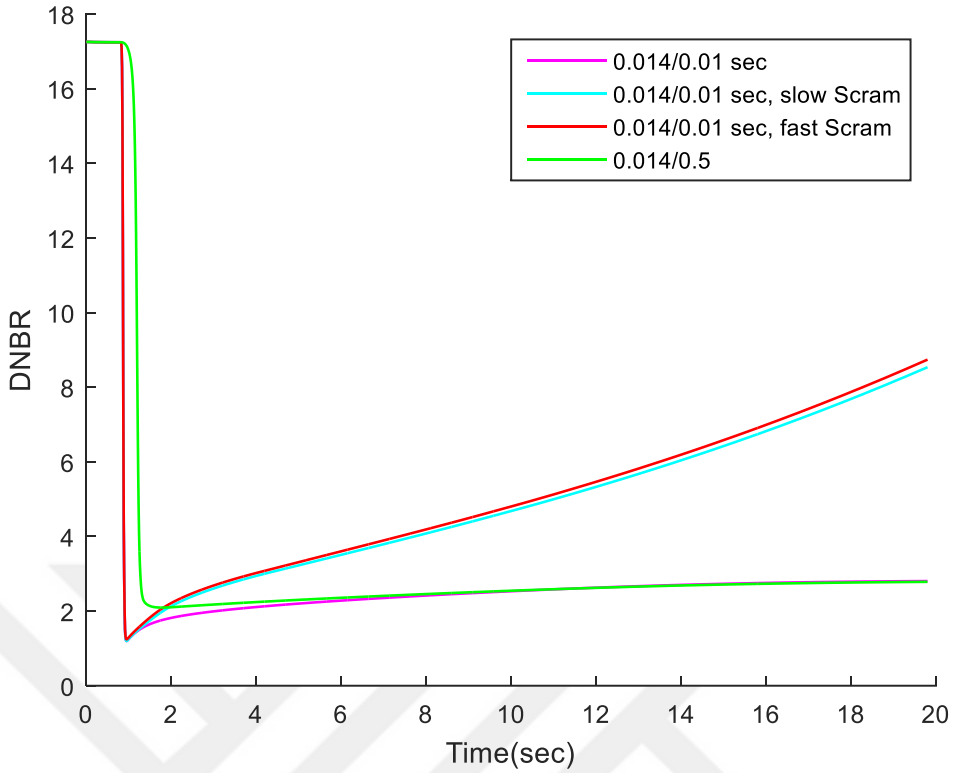

Figure 4.11 : DNBR change vs time at the hottest segment.

For a better insight on the safety performance during the above presented study cases of RIA events, Table 4.1 gives a numerical picture for the safety parameters with respect to each case. Considering that the design limits for TRIGA reactor as mentioned in [15], [16], and [35] for maximum fuel temperature, cladding temperature and minimum DNBR are 1150℃, 500℃ and 1.0, respectively. Therefore, it can be concluded that for all scenarios fuel average temperature and cladding temperature didn't reach the safety limits. However, if the reactor design limits have been pushed for more conservative limits (i.e. to minimum DNBR 1.2), in order to reduce the impact of possible uncertainties. The reactor in case of step reactivity insertion of 0.014/step will still be considered as safe, because the temperature and the minimum DNBR exceeds those limits for a very short time. That wouldn't compromise the safety of the reactor, since no severe consequences has been observed. In addition, it can be seen from Table 4.1 that there is a drastic difference in safety parameters between unprotected and protected cases for reactivity insertion of 0.007/step, However, in case of reactivity insertion of 0.014/step, there is a relatively smaller difference, but it becomes more obvious considering the existence of scram system with small delay. Besides, the average fuel temperature doesn't change much, that can be understood by

observing the fuel temperature behaviors in Figure 4.9. This indicates that the net reactivity is mainly dominant in the beginning of the transient stage by the magnitude of the reactivity insertion. However, that only occurs if the magnitude of the external reactivity is relatively big in comparison to the impact imposed by reactivity feedbacks.

Table 4.1 : Safety analysis results for different RIA scenarios using EUREKA-2/RR.

RIA Scenario	Maximum Power (MW)	Maximum Average Fuel Temperature ℃	Maximum Cladding Temperature ℃	Minimum DNBR
0.0035/step Unprotected	0.6439	106.182	63.0524	11.5551
0.007/step				
Unprotected	3.0977	161.616	85.107	4.5592
Protected	2.9997	80.622	55.0183	8.2158
0.014/step				
Unprotected	453.982	273.047	151.882	1.1969
Protected with 0.1 sec delay	453.982	253.328	151.88	1.197
Protected with 0.01 sec delay	438.213	248.057	150.435	1.2428
Unprotected ramp reactivity 0.014/(0.5 sec)	117.115	259.509	129.475	2.0942

4.2 Safety Analysis Using TM2-RIA

The code TM2-RIA has been used for investigating the steady state behavior and three transient cases of TRIGA Mark II, for different RIA scenarios corresponding to the reactivity insertion rates 0.014/step, 0.007/step, and 0.0035/step. Besides, three different neutronic parameters groups (described as neutronic cases later on for simplicity) have been implemented;

A. Neutronic parameters are taken from [48] for six precursors groups.
B. Neutronic parameters of six groups presented in Table 3.1
C. Neutronic parameters of eight groups presented in Table 3.1

This section presents the results and discuss the capabilities and reliability of TM2-RIA, furthermore, compare it with EUREKA-2/RR code. The kinetics calculations took place at time=1 second till 20 seconds, and all calculations have been demonstrated, considering axial and radial regions are divided into $n_z = 18$ (axial), $n_f = 5$ (radial in the fuel region), $n_{cl} = 3$ (radial in the cladding region). All the results presented in this section are for the hottest slab in the hot channel.

In case of steady-state (operational) analyses, the reactor has been considered operating at operational power 0.25 MW. Besides, the impact of number and size of thermal-hydraulic control volumes (segments) is also studied, by considering 10 and 18 segments. The results which are shown in Figure 4.12, represent the temperature behaviors in the hot channel. The figure shows that in all cases, the coolant temperature profiles have very small deviation, which reaches almost 1℃ at its max as can be seen from Figure 4.12.C. However, more deviations start taking place in hotter regions, where significant gap between centerline temperature profiles as shown in Figure 4.12.A.

It can be concluded that the size and number of segments play role in the temperature profiles, which is expected since the power fraction at each segment differs significantly. Keeping in mind that also number of channels influences that, which may explain why there is still a significant gap between the TM2-RIA (10 segments) and EUREKA-2/RR (10-segments).

However, it is not investigated in this study. Moreover, the TM2-RIA code predicts the initial fields using analytical solutions, which is advantage over the explicit numerical method adapted in EUREKA-2/RR code. That being said, comparing its performance to another code that applies the same concept in extracting the initial fields (such as; COOLOD-N2), would be helpful in justifying TM2-RIA reliability in computing the initial state.

A)

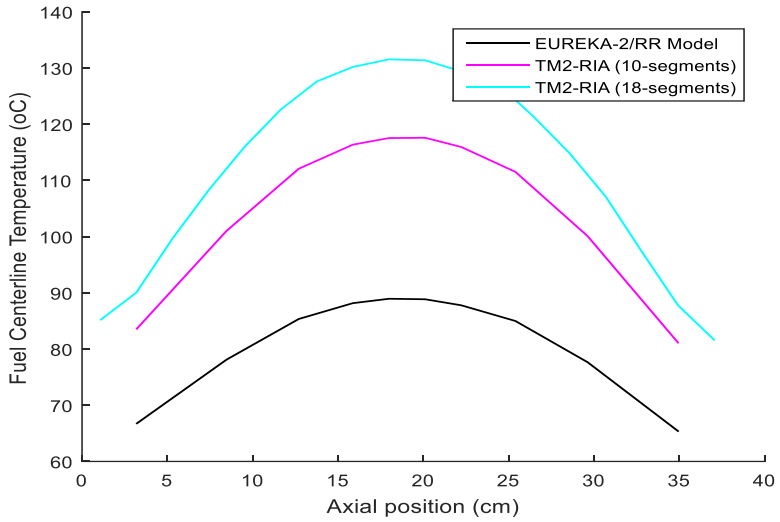

B)

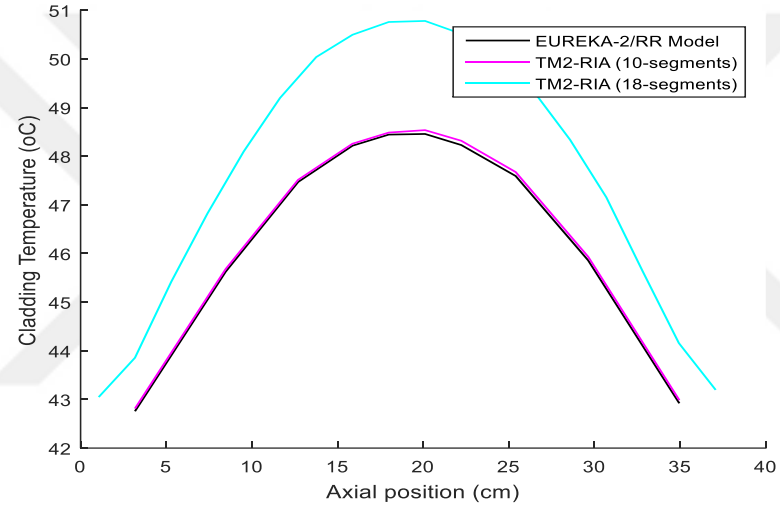

C)

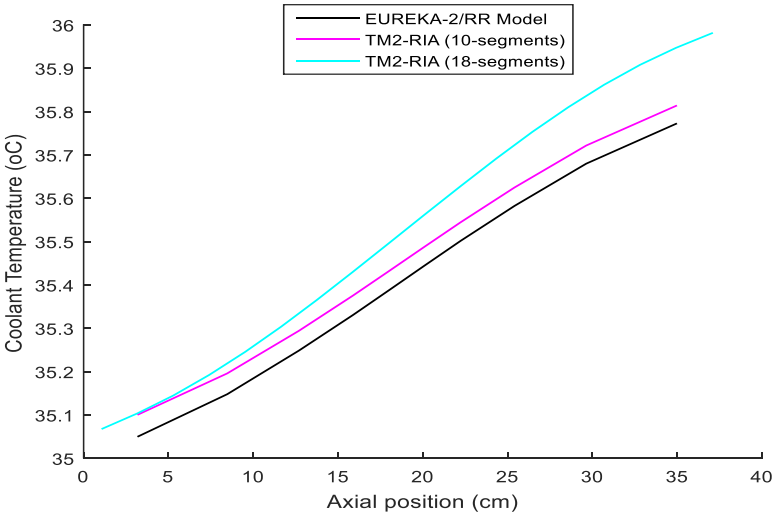

Figure 4.12 : Axial temperature profiles; A) fuel centerline, B) cladding surface, and C) coolant in hot channel. At steady-state (0.25 MW) based on the code, size and number of control volumes applied.

For the first RIA scenario; in general, Figure 4.13 shows how both ITU TRIGA Mark II model developed by EUREKA-2/RR and TM2-RIA are in good agreement. However, there is a very small shift in time of peak power occurrence, and both neutronic cases (B) and (C) reached much lower peak power levels, less than 440 MW and 410 MW, respectively.

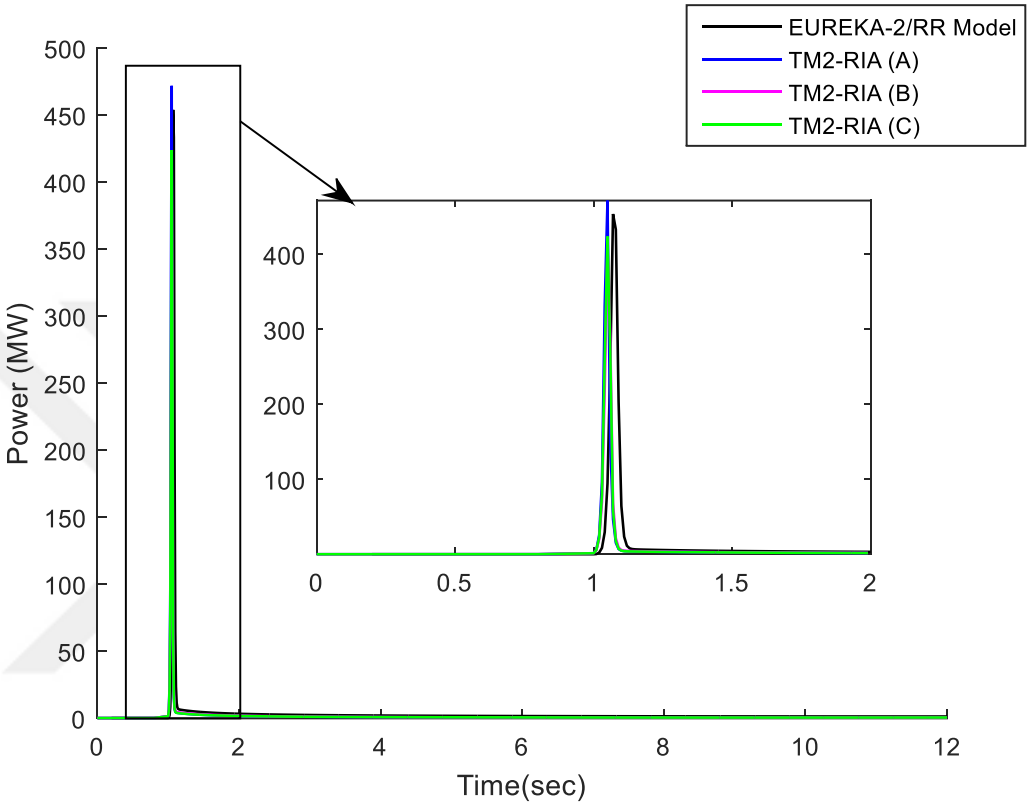

Figure 4.13 : Power vs time, using the results extracted from EUREKA-2/RR code and TM2-RIA for 3 different neutronic cases.

The deviation between TM2-RIA models and EURKEA-2/RR model are relatively minor at early stage of reactor kinetics. Besides, it is hard to observe the neutronic cases influence in this scenario, in changing the behavior of the reactor transient response. That being said, the TM2-RIA model drop rates behaviors shown in Figure 4.14, are quite different from what is produced by EUREKA-2/RR model. The TM2-RIA models reach less than 100℃ while EUREKA-2/RR model reaches more than 120℃ at 12 second. The source behind this difference can be understood by investigating the coolant temperature, which can be observed in Figure 4.15. Even though both codes showed similar trends, the gap between two parallel points are enough to cause significant change in the heat transfer behavior, since the heat coefficient values will be different.

That can be attributed to the difference between the codes in solving the energy equation numerically. Furthermore, it can be attributed to the methodology adapted in calculating the reactivity feedbacks, where the latter is related to number and size of control volumes (segments), heat coefficient calculations.

This difference in behavior is reflected in the prediction of DNBR values as shown in Figure 4.16, where it can be seen that the TM2-RIA models produced a sloppier increment than what is produced by EUREKA-2/RR model. In addition, DNBR results from TM2-RIA start around 13.5, whereas in the latter it starts around 17. This is a result of the initial fields evaluation difference between the two codes as discussed previously. That being said, all trends of the discussed results are in good agreement, and the safety limits are satisfied at almost the same magnitudes, which will be discussed more later on.

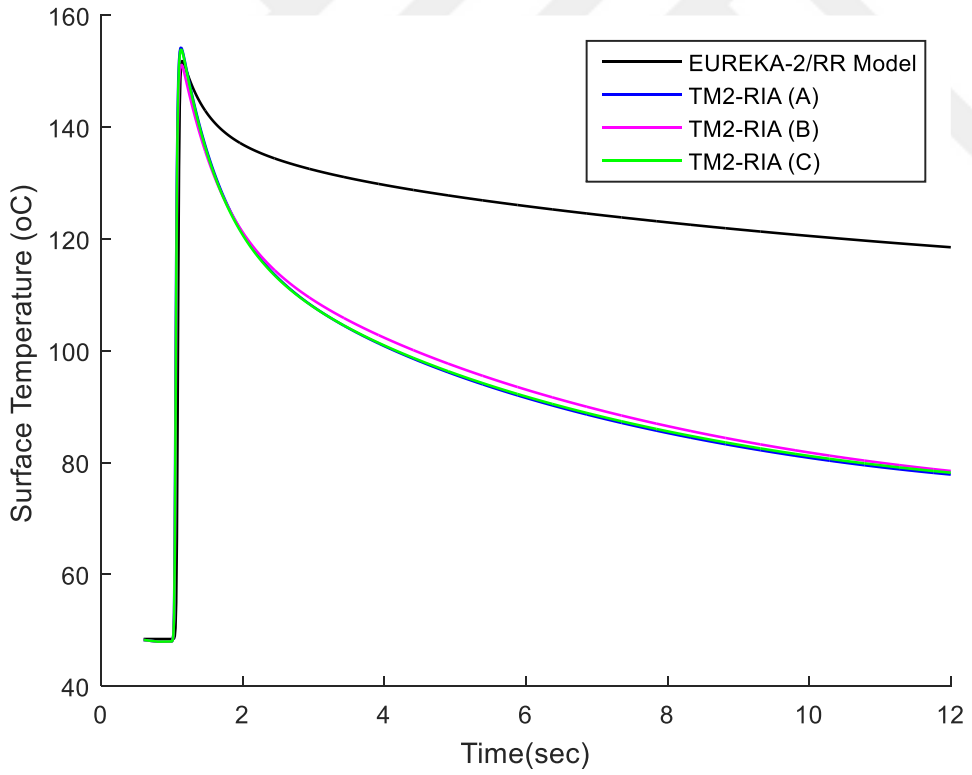

Figure 4.14 : Cladding surface temperature vs time at the hottest segment, using the results extracted from EUREKA-2/RR code and TM2-RIA for 3 different neutronic cases.

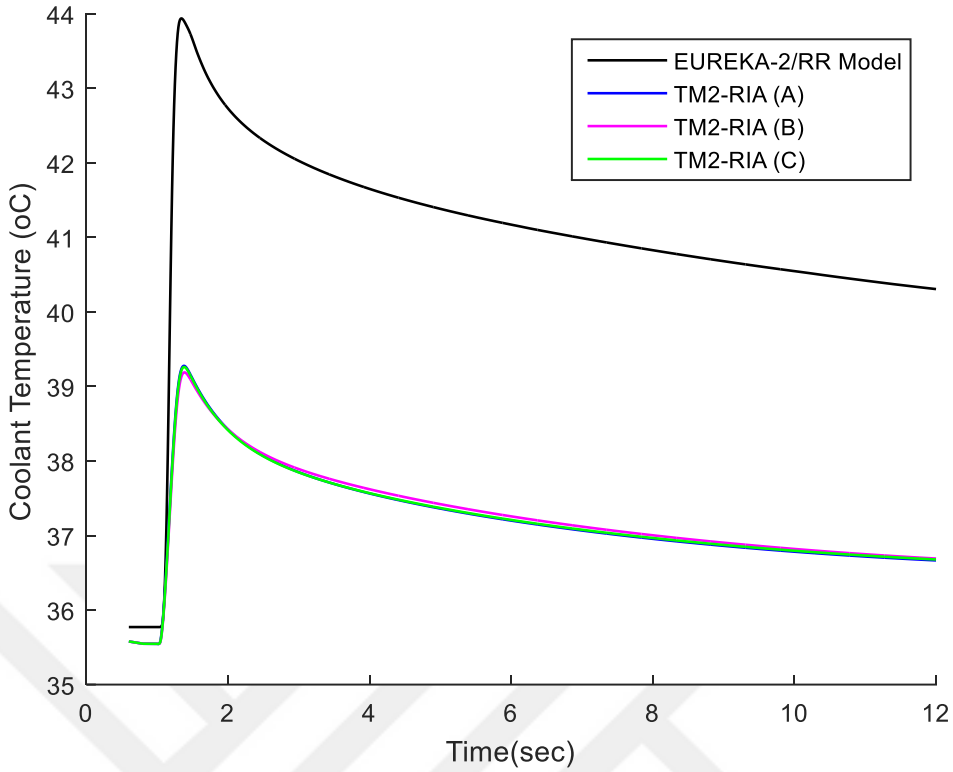

Figure 4.15 : Coolant Temperature at exit of hot channel vs time, using the results extracted from EUREKA-2/RR code and TM2-RIA for 3 different neutronic cases.

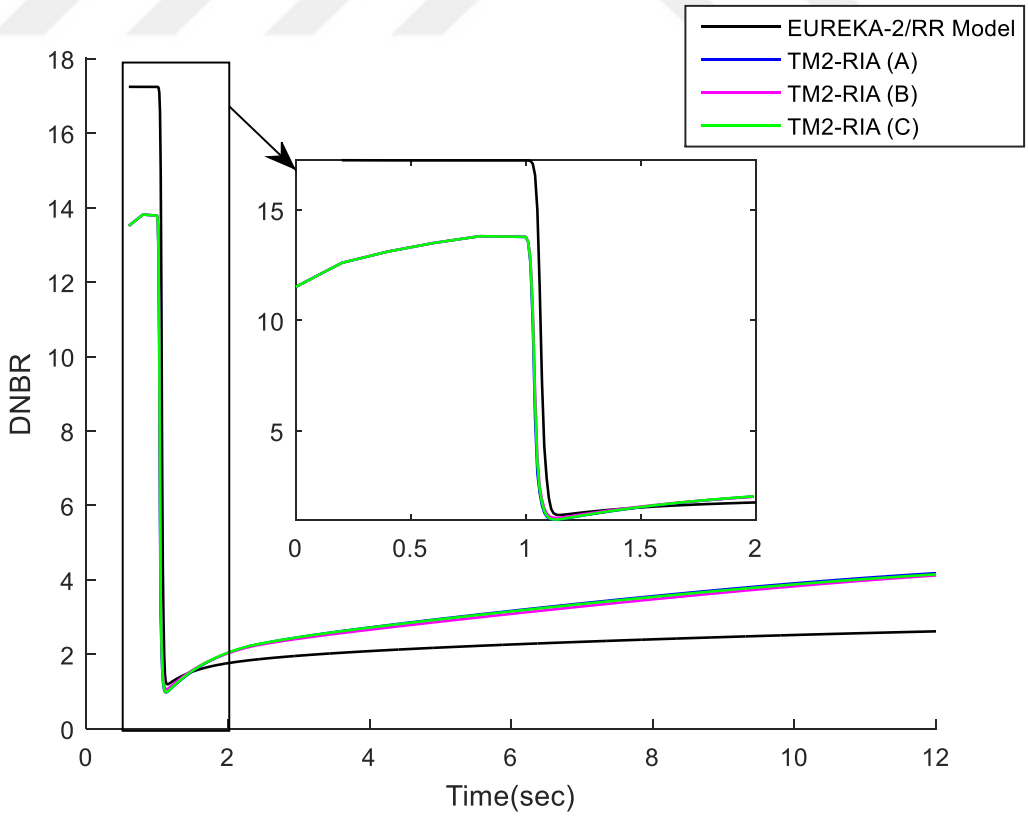

Figure 4.16 : DNBR change vs time at the hottest segment, using the results extracted from EUREKA-2/RR code and TM2-RIA for 3 different neutronic cases.

In the second RIA scenario (0.007/step), the impact of implementing different neutronic cases is more pronounced as shown in Figure 4.17. Thus, it can be said that the magnitude of reactivity insertion has role in eclipsing or enhancing the effect of the adapted neutronic case. That being said, it seems easy to say that the neutronic case (B) shows closest performance to the EUREKA-2/RR model, but it is not the case from the results shown in Figure 4.18, in which case (A) seems to perform better. This makes it not easy to judge which group performed the closest to the EUREKA-2/RR model.

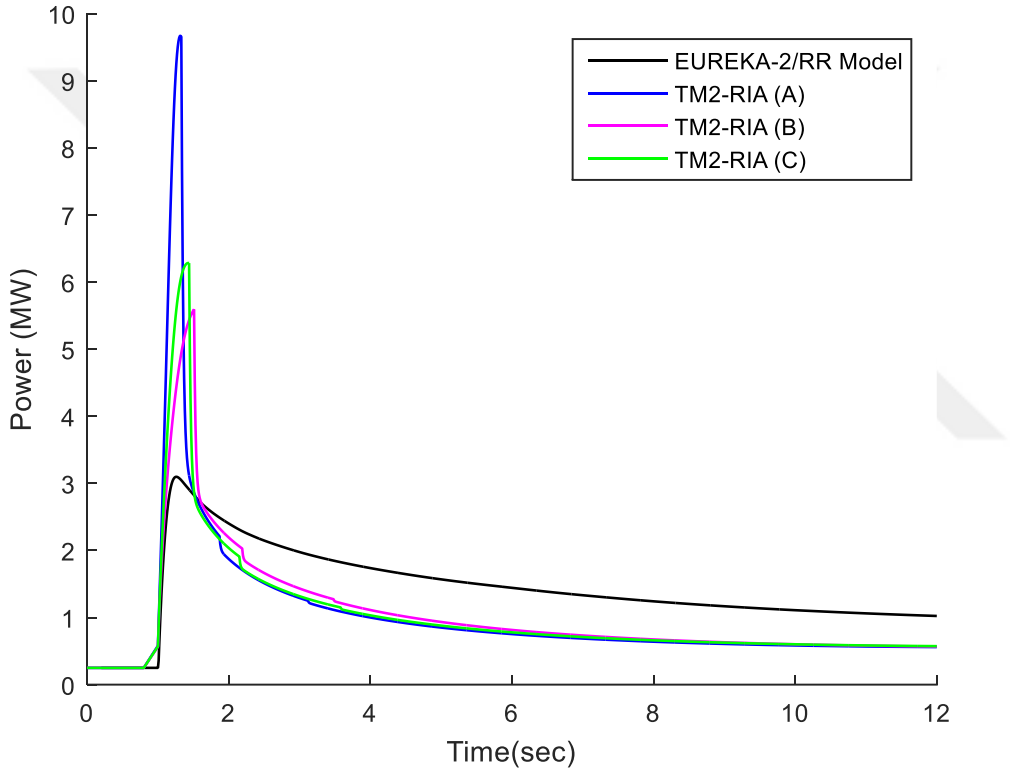

Figure 4.17 : Power vs time, using the results extracted from EUREKA-2/RR code and TM2-RIA for 3 different neutronic cases.

The rapid raise in power and fast drop afterword in case of TM2-RIA models, explain the behaviors shown in Figure 4.18 till Figure 4.20. Where it can be seen that peak temperatures and minimum DNBR are reached faster, then a slow decrease in temperature starts taking place. Meanwhile, in case of EUREKA-2/RR temperatures and DNBR values are increasing and decreasing, respectively. The reason behind that is similar to what has been discussed in the previous section in case of slow and fast RIA events.

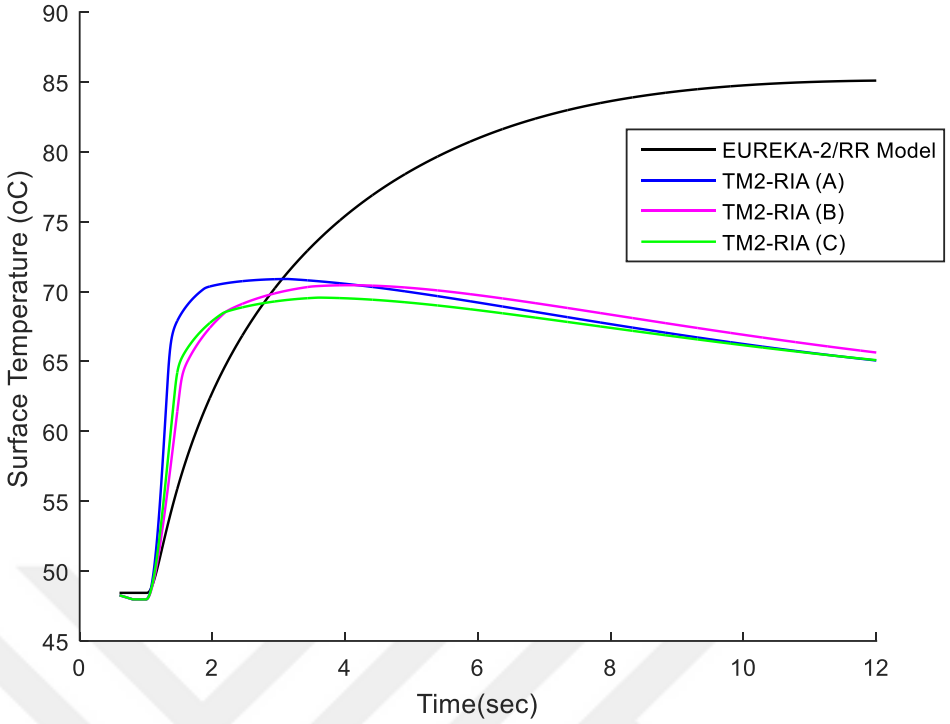

Figure 4.18 : Cladding surface temperature vs time at the hottest segment, using the results extracted from EUREKA-2/RR code and TM2-RIA for 3 different neutronic cases.

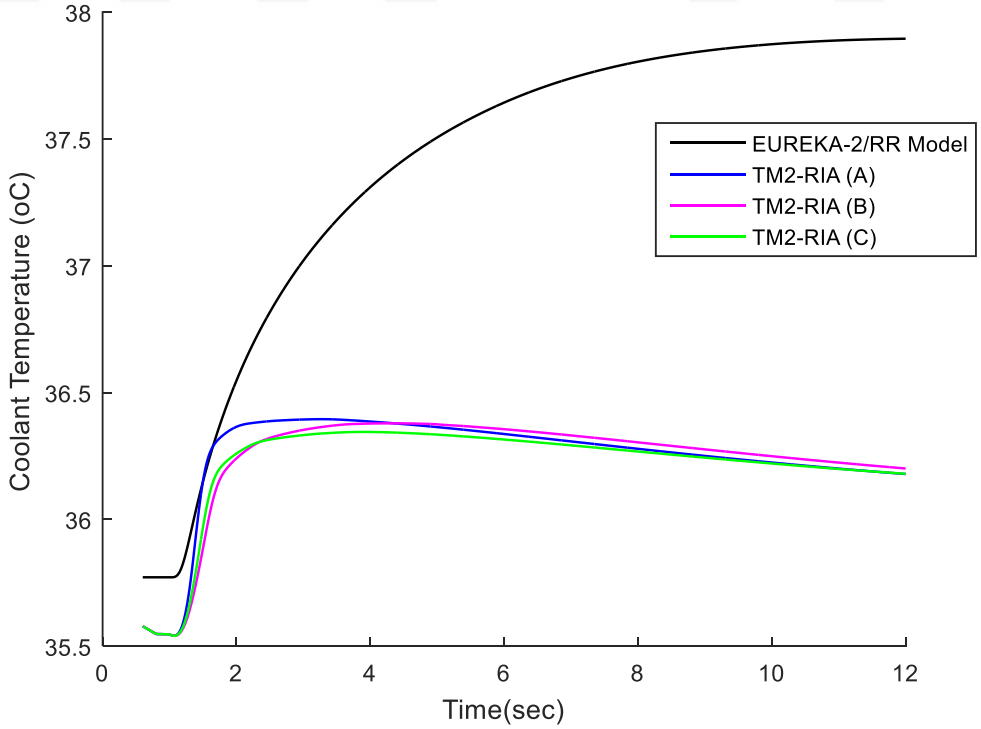

Figure 4.19 : Coolant Temperature at exit of hot channel vs time, using the results extracted from EUREKA-2/RR code and TM2-RIA for 3 different neutronic cases.

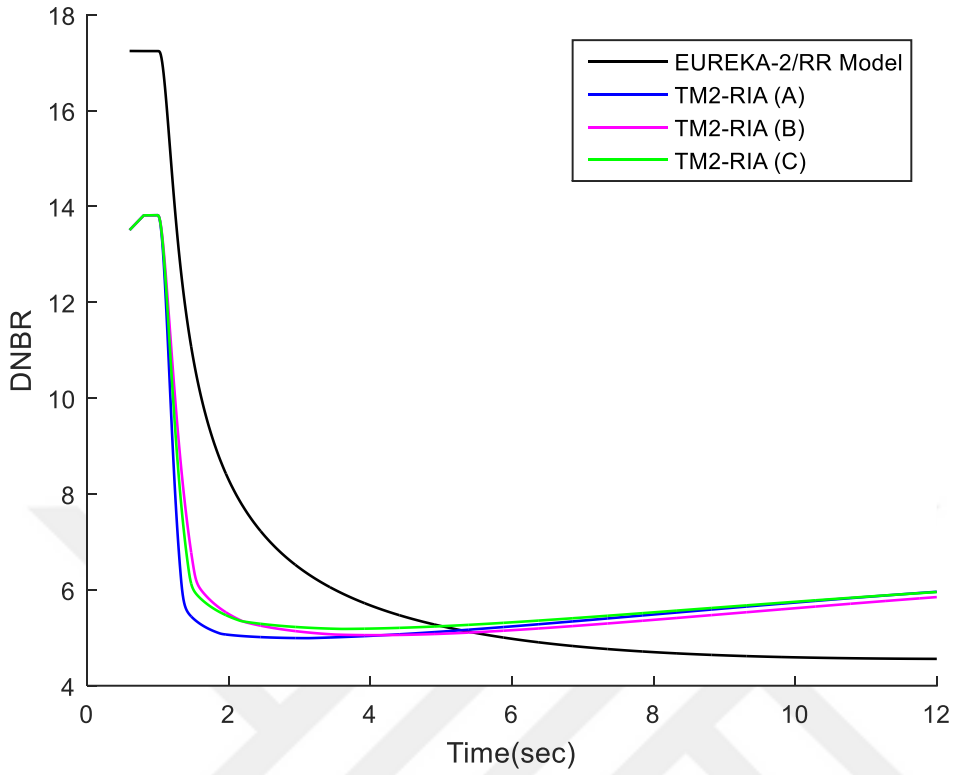

Figure 4.20 : DNBR change vs time at the hottest segment, using the results extracted from EUREKA-2/RR code and TM2-RIA for 3 different neutronic cases.

When it comes to the third RIA scenario, the implemented neutronic case influences more significantly, the trends of the power shape introduced in Figure 4.21 are clearly different than what is produced by EUREKA-2/RR model. TM2-RIA model produces obvious peaks and strong power drops afterwards, which EUREKA-2/RR doesn't show that behavior. In addition, the neutronic cases influence can be also seen in terms of the time location at which peak powers are reached. The unexpected and strong slope in power trend has affected the reactor thermal behavior in a similar manner, as shown in Figure 4.22 and Figure 4.23, which is surely reflected in DNBR change as shown in Figure 4.24. The disagreement related to the performance of TM2-RIA and EUREKA-2/RR in this concerned scenario, imposes the need of improvements in order for TM2-RIA to cover RIA events with low reactivity insertion rates.

This can be done by considering adapting different point kinetic solution method, which was proved to be reliable in such events. For example; singularly perturbed method highlighted in Section 2, can be a good candidate as a start.

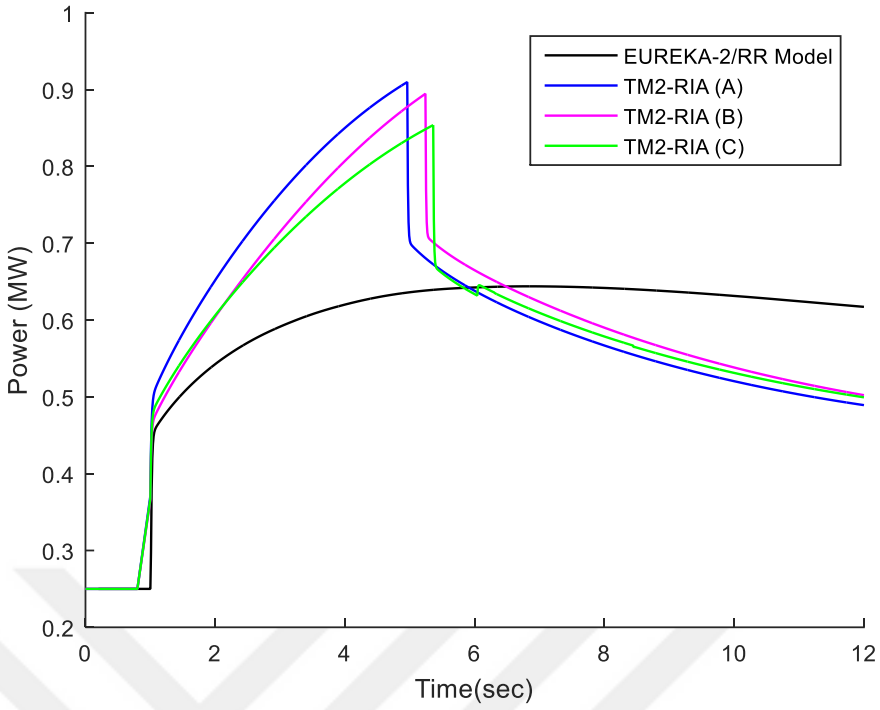

Figure 4.21 : Power vs time, using the results extracted from EUREKA-2/RR code and TM2-RIA for 3 different neutronic cases.

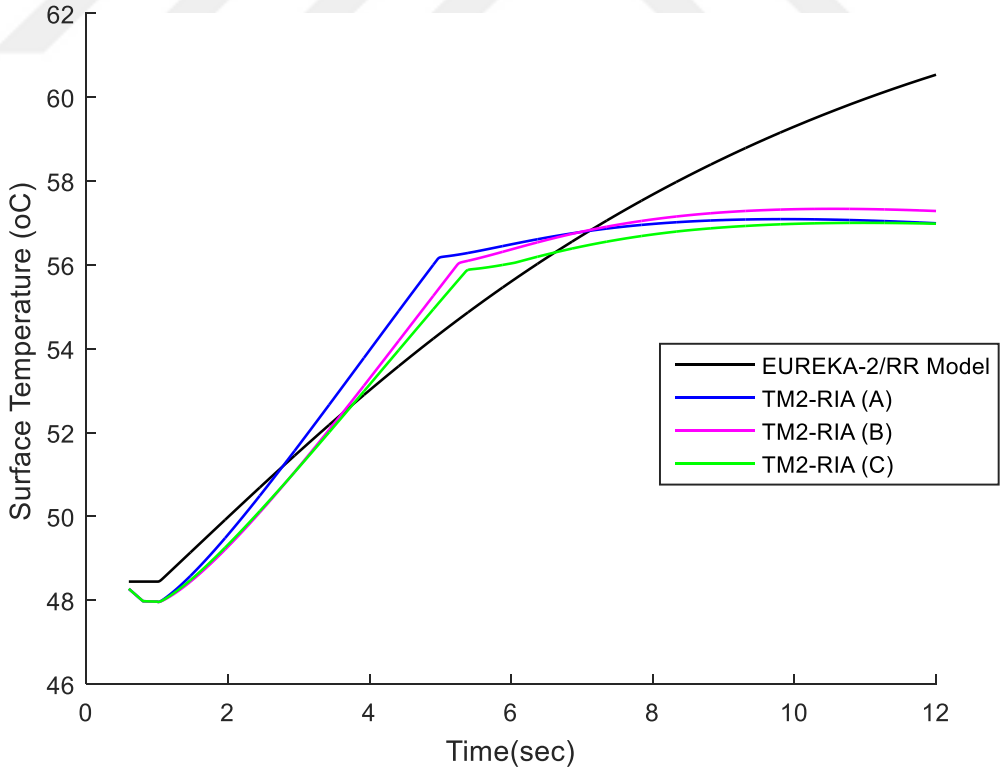

Figure 4.22 : Cladding surface temperature vs time at the hottest segment, using the results extracted from EUREKA-2/RR code and TM2-RIA for 3 different neutronic cases.

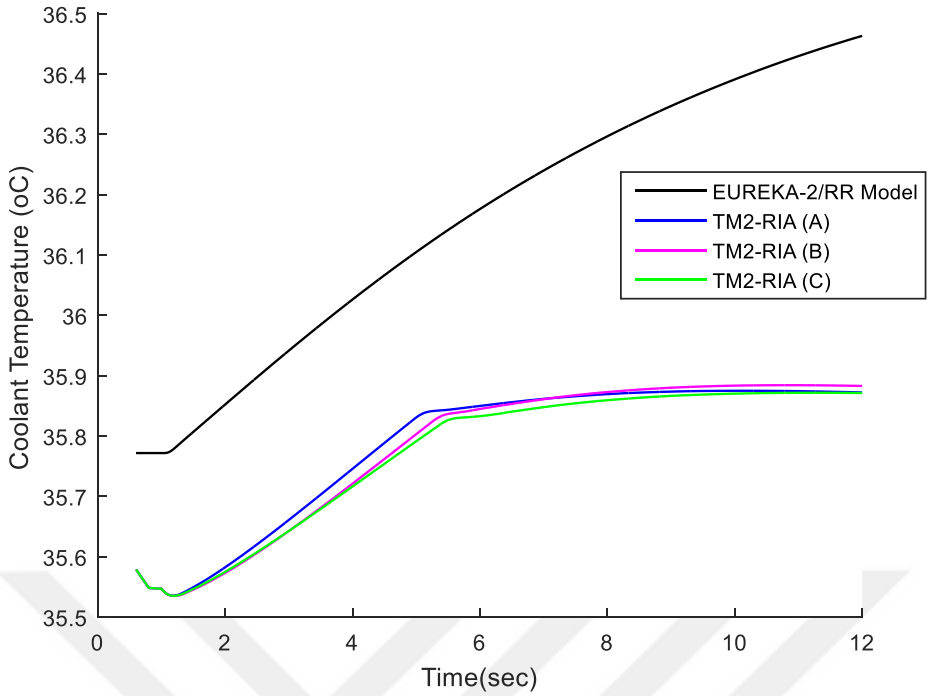

Figure 4.23 : Coolant Temperature at exit of hot channel vs time, using the results extracted from EUREKA-2/RR code and TM2-RIA for 3 different neutronic cases.

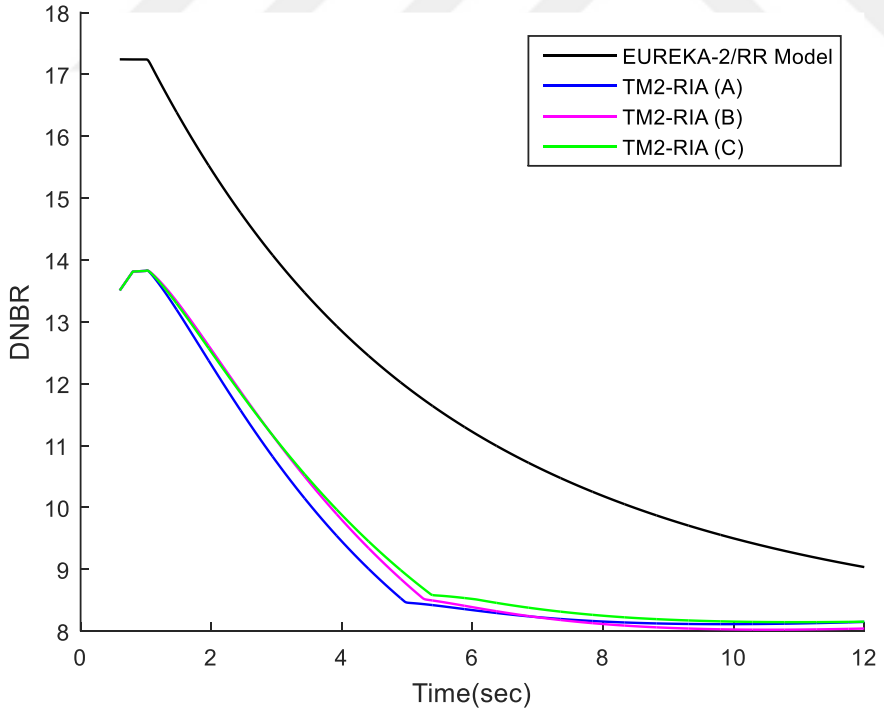

Figure 4.24 : DNBR change vs time at the hottest segment, using the results extracted from EUREKA-2/RR code and TM2-RIA for 3 different neutronic cases.

Table 4.2 gives insight on the numerical performance of the discussed models regarding some of the safety parameters. Initially it was expected that TM2-RIA (A)

would have performed the closest to the EUREKA-2/RR model, since the neutronic case is the same. That haven't been the case in all RIA scenarios, which indicates that the point kinetics solution adapted influences the associated neutronic parameters attributes. Besides, each neutronic case implemented in TM2-RIA hasn't shown a consistent performance corresponding to the three RIA scenarios. However, the results show the importance of implementing the accurate set of neutronic parameters. That can be observed by taking case (A) as the reference, and evaluating the maximum relative differences of the calculated power corresponding to RIA (i.e., in case of 0.0035/step: (0.9096-0.8536)/0.9096)). The relative differences from the lowest to the highest reactivity insertion are found to be; (6%, 42% and 13%). RIA analyses of all cases using both codes ensure the safety of the reactor as can be concluded from Table 4.2. Although, TM2-RIA models have reached a minimum DNBR less than 1.0, however, the reactor reaches this state for a very short time leading into no critical consequences.

Table 4.2 : Comparison of safety design limits for different models.

Study Case	Maximum Power (MW)	Maximum Cladding Temperature ℃	Minimum DNBR
0.0035/step			
EUREKA-2/RR	0.6439	63.0524	11.5551
TM2-RIA (A)	0.9096	57.086	8.1168
TM2-RIA (B)	0.8944	57.332	8.027
TM2-RIA (C)	0.8536	56.8125	8.2185
0.007/step			
EUREKA-2/RR	3.0977	85.107	4.5592
TM2-RIA (A)	9.671	70.8994	4.9933
TM2-RIA (B)	5.5932	70.455	5.0558
TM2-RIA (C)	6.2837	69.567	5.1856
0.014/step			
EUREKA-2/RR	453.982	151.882	1.1969
TM2-RIA (A)	471.916	154.26	0.9083
TM2-RIA (B)	409.56	151.189	1.063
TM2-RIA (C)	423.964	153.9418	0.9885

5. CONCLUSIONS AND RECOMMENDATIONS

A multi-physics model of ITU TRIGA Mark II has been developed using EUREKA-2/RR code and introduced in this study. The model has been used for safety analysis of seven different RIA events. Furthermore, a completely original code (TM2-RIA) has been developed for TRIGA Mark II with cylindrical fuel type for simulating the reactor at steady-state and transient behaviors, also able to analyze the RIA scenarios consequences. The adapted methodologies and algorithm all have been addressed.

The safety analyses performed by EUREKA-2/RR model have shown how significant can be the impact of the reactivity insertion rate, in case of 0.0035/step the peak power has reached 0.6439 MW, whereas, in case of 0.014/step it has reached 453.982 MW. The influence of scram hasn't been significant in the early stages of reactor kinetics, especially when delay is long (0.1 sec), in which the same power in unprotected case has been observed. While in case of fast delay (0.01 s) peak power has been 438.213 MW. On the other hand, in case of 0.007/step, the reactor's power drops to almost 1.5 MW in less than one second. Also there have been more than 80℃ and 30℃ differences in maximum fuel and cladding surface temperatures, respectively. The protected cases have produced strong negative total reactivity, resulting into a sloppy and a fast increment in the DNBR change trend after it reaches its minimum values, which ensures the safety of the reactor to overcome possible consequences.

Moreover, the investigation of slow reactivity insertion of 0.014 per 0.5 sec has produced shifting in peak power occurrence (0.35 seconds after the step reactivity insertion case) and a low magnitude of power (~117 MW). However, there is no much difference in the temperatures transient behavior, but the peak fuel temperatures are at very different time locations.

It has been concluded that the EUREKA-2/RR ensures ITU TRIGA Mark II safe responses for all the presented cases, since all values are inside the safety margins. It is found that the highest and lowest evaluated cladding surface temperature and DNBR (151.882℃, and 1.1969), respectively. Moreover, the reactor resides at this critical state for a very short time, leading into no aggravated consequences as the results have

indicated. That ensures the safety of the reactor, even for more conservative design limits.

By the comparison of TM2-RIA and EUREKA-2/RR models results, it is observed that TM2-RIA has the advantage in calculating the steady-state parameters analytically and implementing them to initiate the transient analysis. Besides, it has another advantage for giving the freedom in applying the neutronic parameters, which leads to more possibilities in utilizing it. Moreover, the possibility of modifying it to include different thermal-hydraulic structure, when it comes to number of channels, control volumes and their sizes. It has been proved in this study, how the thermal-hydraulic adapted scheme (channels and segments) is a factor in predicting the operational state parameters.

It has been observed through the steady-state thermal-hydraulic analysis, that there is no issue at all with the presented results when it comes to safe operation. The transient analyses also show the significance of implementing the accurate set of neutronic parameters, especially on the critical values of safety parameters. That has been investigated by considering the neutronic parameters presented in [48] to be the reference for 0.0035/step, 0.007/step and 0.014/step, and evaluating the relative difference in peak power, which are found to be (6%, 42% and 13%), respectively. In addition, the influence left prints in terms of the temporal location (in some cases time difference is more than 0.5 seconds). That being said, EUREKA-2/RR has been much superior in covering a wider range of RIA events.

The promising performance of TM2-RIA and the conducted safety analyses with both codes open many doors for future works. However, since differences have been observed, modeling using a third common code for research reactors (such as PARET) would be quite helpful in understanding the positions of the developed models used in this study. Certainly, there are room for improvements of TM2-RIA to cover RIA scenarios with relatively low reactivity insertion rates, that can be initiated by developing different point kinetics solution method (such as; singularly perturbed method).

In order to improve the TM2-RIA code to be more generic and robust, including different heat transfer packages to give and extending the code to cover regions beyond subcooled nucleate boiling. Development of a flow inversion model based on some of

the highlighted literature in Section 1 is required for LOFA scenarios. However, to remove the restrictions faced by previous studies regarding the flow loss percentage that can be analyzed, developing two phase flow model is recommended.

Finally, further works can be done in extending the capabilities of TM2-RIA in modelling the commercial reactors of ATMEA and VVER-1200 type, which are expected to be the next future reactors for the nuclear energy in Turkey.

REFERENCES

[1] **R. K. McCurdell, D. I. Herborn and J. E. Houghtaling,** "Reactivity accident tests results and analyses for the SPERT III e-core a small oxide-fueled, pressurized water reactor," US Atomic Energy Comissioner, Report, IDO-17281, doi:10.2172/4792676, March 1969.

[2] **J. G. Crocker and L. A. Stephan,** "Reactor power excursion tests in the spert iv facility," US Atomic Energy Comission, ID0-17000 , August 1964.

[3] **M. Margulis and E. Gilad,** "Simulations of SPERT-IV D12/15 transient experiments using the system code THERMO-T," *Progress in Nuclear Energy,* vol. 109, pp. 1-11, 2019.

[4] **A. Dokhane, G. Grandi, A. Vasiliev, D. Rochman and H. Ferroukhi,** "Validation of PSI best estimate plus uncertainty methodology against SPERT-III reactivity initiated accident experiments," *Annals of Nuclear Energy,* vol. 118, pp. 178-184, 2018.

[5] **C. Stewart et al.,** "COBRA-IV: the model and the method," BNWL-2214, NRC-4, July 1977.

[6] **M. Kaminaga,** "EUREKA-2/RR: a computer code for the reactivity accident analyses in research reactors," Japan Atomic Energy Agency, 2017.

[7] **C. Obenchain,** "PARET: a program for the analysis of reactor transients," AEC Research and Development Report IDO-17282, 1969.

[8] **M. Kaminaga,** COOLOD-N2: a computer code for the analysis of steady-statethermal-hydraulics in research reactors, Japan: Japan Atomic Research Institute, 1994.

[9] **W. L. Woodruff, N. A. Hanan, R. S. Smith and J. E. Matos,** "A comparison of the PARET/ANL and RELAP5/MOD3 codes for the analysis of iaea benchmark transients," in *International Meeting on Reduced Enrichment for Research and Test Reactors*, Seoul, Korea, 1996.

[10] **G. Thelera and D. Freisb,** "Theoretical critical heat flux prediction based on non-equilibrium thermodynamics considerations of the subcooled boiling phenomenon," in *Asociación Argentina de Mecánica Computacional November 1-4*, Rosario, Argentina, 2011.

[11] **D. Schroeder-Richter and G. Bartsch,** "Analytical calculation of DNB-superheating by a postulated thermo-mechanical effect of nucleate boiling," *International Journal of Multiphase,* vol. 20, no. 6, p. 1143–1167, 1994.

[12] **Y. Guo, G. Wang, D. Qian, H. Yu, B. Hu, S. Guo and X. Mi,** "Thermal hydraulic analysis of loss of flow accident in the JRR-3M research reactor under the flow blockage transient," *Annals of Nuclear Energy,* vol. 118, pp. 147-153, 2018.

[13] **Y. Guo, G. Wang, D. Qian, H. Yu, B. Hu, S. Guo, X. Mi and J. Ma,** "Accident safety analysis of flow blockage in an assembly in the JRR-3M research reactor using system code RELAP5 and CFD code FLUENT," *Annals of Nuclear Energy,* vol. 122, pp. 125-136, 2018.

[14] **Y. Boulaich, B. Nacir, T. El-Bardouni, H. Boukhal, E. Chakir, B. El-Bakkari and C. El-Younoussi,** "Transient behavior during reactivity insertion in the Moroccan TRIGA Mark II reactor using the PARET/ANL code," *Nuclear Engineering and Design,* vol. 284, pp. 247-250, 2015.

[15] **P. M. Babitz,** Thermohydraulics analysis of the university of utah triga reactor of higher power designs, Salt Lake City, UT, USA: Department of Civil and Environmental Engineering, The University of Utah, December 2012.

[16] **N. Badrun, M. Altaf, M. Khan, M. Mahmood, M. Motalab and Z. Lyric,** "Thermal hydraulic transient study of 3MW TRIGA Mark-II research reactor of Bangladesh using the EUREKA-2/RR code," *Annals of Nuclear Energy,* vol. 41, pp. 40-47, 2012.

[17] **M. Altaf, S. T. Islam and N. Badrun,** "RIA analysis of unprotected TRIGA reactor," *Atom Indonesia,* Vols. 43-2, pp. 69-73, 2017.

[18] **B. N. Hamid, M. A. Hossen, S. Md, T. Islam and R. Begum,** "Modelling an unprotected loss-of-flow accident in research reactors using the Eureka-2/Rr Code," *Journal of Physical Science,* vol. 26(2), pp. 73-87, 2015.

[19] **M. Kaminaga,** "EUREKA-2/RR input data for jrr-3m reactivity initiated events analysis," Japan Atomic Energy Agency, 2017.

[20] **X. Shen, K. Nakajima, H. Unesaki and K. Mishima,** "Reactivity insertion transient analysis for KUR low-enriched uranium silicide fuel core," *Annals of Nuclear Energy,* vol. 62, pp. 195-207, 2013.

[21] **T. Hamidouche, A. Bousbia-Salah, E. Si-Ahmed and F. D'Auria,** "Overview of accident analysis in nuclear research reactors," *Progress in Nuclear Energy,* no. 50, pp. 7-14, 2008.

[22] **C. Housiadas,** "Lumped parameters analysis of coupled kinetics and thermal-hydraulics for small reactors," *Annals of Nuclear Energy,* vol. 29, pp. 1315-1325, 2002.

[23] **H. Kazeminejad,** "Thermal-hydraulic modeling of flow inversion in a research reactor," *Annals of Nuclear Energy*, vol. 35, pp. 1813-1819, 2008.

[24] **M. Margulis and E. Gilad,** "Analysis of protected ria and lofa in plate type research reactor using coupled neutronics thermal-hydraulics system code," in *NURETH-16, Chicago, IL, August 30-September 4*, Chicago, IL, 2015.

[25] **A. Bousbia-Salah and T. Hamidouche,** "Analysis of the IAEA research reactor benchmark problem by the RETRAC-PC code," *Nuclear Engineering and Design*, no. 235, pp. 661-674, 2005.

[26] **H. Kazeminejad,** "Thermal-hydraulic modeling of reactivity insertion in a research reactor," *Annals of Nuclear Energy*, no. 45, pp. 59-67, 2012.

[27] **T. Mazumdar, T. Singh, H. P. Gupta and K. Singh,** "RITAC: reactivity initiated transient analysis code," *Annals of Nuclear Energy,* vol. 43, pp. 192-207, 2012.

[28] **S. E. El-Morshedy,** "Thermal-hydraulic modeling and analysis of a tank in pool reactor for normal operation and loss of flow transient," *Progress in Nuclear Energy,* vol. 61, pp. 78-87, 2012.

[29] **R. Henry, I. Tiselj and L. Snoj,** "CFD/Monte-Carlo neutron transport coupling scheme, application to TRIGA reactor," *Annals of Nuclear Energy,* vol. 110, pp. 36-47, 2017.

[30] J**. Chen, T. Zhou, L. Liu and X. Fang,** "Analysis on LOCA for CSR1000," *Annals of Nuclear Energy,* vol. 110, pp. 903-908, 2017.

[31] **R. Sun, D. Zhang, Y. Liang, M. Wang, W. Tian, S. Qiu and G. Su,** "Development of a subchannel analysis code for SFR wire-wrapped fuel assemblies," *Progress in Nuclear Energy,* vol. 104, pp. 327-341, 2018.

[32] **C. Hellesen and S. Qvist,** "Benchmark and demonstration of the CHD code for transient analysis of fast reactor systems," *Annals of Nuclear Energy,* vol. 109, pp. 712-719, 2017.

[33] **A. Arkoma,** "Extending the reactivity initiated accident (RIA) fuel performance code SCANAIR for boiling water reactor (BWR) applications," *Nuclear Engineering and Design*, vol. 322, pp. 192-203, 2017.

[34] **W. R. Marcum, T. S. Palmer, B. G. Woods, S. T. Keller and S. R. Reese,** "A comparison of pulsing characteristics of the oregon state university triga reactor with FLIP and LEU fuel," *Nuclear Science And Engineering,* vol. 171, pp. 150-164, 2012.

[35] **G. A. GA,** "Safety analysis report of ITU TRIGA Mark II," Energy Institute, Istanbul Technical University, Istanbul, 1979.

[36] **J. J. Szeligowski,** Numerical methods for solving the reactor kinetics equations, Tucson, Arizona, USA: The University of Arizona, 1966.

[37] **J. Sánchez,** "On the numerical solution of the point reactor kinetics equations by generalized runge-kutta methods," *Nuclear Science and Engineering,* vol. 103, pp. 94-99, 1989.

[38] **P. Kaps and P. Rentrop,** "Generalized Runge-Kutta methods of order four with stepsize control for stiff ordinary differential equations," *Numer. Math.,* vol. 33, pp. 55-68, 1979.

[39] **A. A. Nahla,** "Taylor's series method for solving the nonlinear point kinetics equations," *Nuclear Engineering and Design,* vol. 241, pp. 1592-1595, 2011.

[40] **W. Chen, J. Hao, L. Chen and H. Li,** "Solution of point reactor neutron kinetics equations with temperature feedback by singularly perturbed method," *Science and Technology of Nuclear Installations,* vol. 2013, pp. xx-xx, 2013.

[41] **M. Kinard and E. Allen,** "Efficient numerical solution of the point kinetics equations in nuclear reactor dynamics," *Annals of Nuclear Energy,* vol. 31, pp. 1039-1051, 2004.

[42] **T. Singh, J. Kumar, T. Mazumdar and V. K. Raina,** "Development of neutronics and thermal hydraulics coupled code SAC-RIT for plate type fuel and its application to reactivity initiated transient analysis," *Annals of Nuclear Energy,* vol. 62, pp. 61-80, 2013.

[43] **A. M. Miraz, S. Khanam and N. M. Miraz,** "Simulation of reactivity transients in current mtrs," *Annual Nuclear Energy ,* vol. 25, pp. 1465-1484, 1998.

[44] **M. Türkmen and Ü. Çolak,** "Analysis of ITU TRIGA Mark II research reactor using Monte Carlo method," *Progress in Nuclear Energy,* pp. 152-159, 2014.

[45] **M. Türkmen, Ü. Çolak and Ş. Ergün,** "Effect of burnup on the neutronic parameters of ITU TRIGA Mark II research reactor," *Progress in Nuclear Energy,* pp. 26-34, 2015.

[46] **J. Leppänen, M. Pusa, T. Viitanen, V. Valtavirta and T. Kaltiaisenaho,** "The Serpent Monte Carlo code: status, development and applications in 2013," *Ann. Nucl. Energy,* p. 142–150, 2015.

[47] **X.-5. M. C. Team,** "MCNP - version 5, vol. i: overview and theory," 2003, Ed., LA-UR-03-1987, 2003.

[48] **Y. Chao and A. Attard,** "A resolution to the stiffness problem of reactor kinetics," *Nuclear Science and Engineering,* vol. 90, pp. 40-46, 1985.

[49] **Y. NAUCHI and T. KAMEYAMA,** "Development of calculation technique for iterated fission probability and reactor kinetic parameters using continuous-

energy Monte Carlo method," *Journal of NUCLEAR SCIENCE and TECHNOLOGY*, vol. 47, no. 11, pp. 977-990, 2010.

[50] **Y. Qiu, Z. Wang, K. Li, Y. Yuan, K. Wang and M. Fratoni,** "Calculation of adjoint-weighted kinetic parameters with the Reactor Monte Carlo code RMC," *Progress in Nuclear Energy*, vol. xxx, pp. 1-11, 2017.

[51] **D. Saengchantr and N. Onishi,** Analysis of steady-state and transient behavior on trr-1/m1 with computer codes coupled neutronic thermal-hydraulic model, Bangkok: Office of Atoms for Peace .

[52] **J. C. Thanehill, D. A. Anderson and R. H. Pletcher,** Computational fluid mechanics and heat transfer series in computational methods in mechanics and Thermal Sciences, New York: Hemisphere Publishing Corporation, 1984.

[53] **A. E. Bergles and W. M. Roshenow,** "The determination of forced convection surface boiling heat transfer," in *6th National Heat Transfer Conference of the ASME-AlChE*, Boston, 11–14th August., 1963.

[54] **T. L. Bergman, A. S. Lavine, F. P. Incropera and D. P. Dewitt,** fundementals of heat and mass transfer, Seventh Edition, United States of America: John Wiley and Sons, 2011.

[55] **B. R. Munson, D. F. Young, T. H. Okiishi and W. W. Huebsch,** Fundementals of Fluid Mechanics, Sixth Edition, United States of America: John Wily & Sons, 2009.

[56] **N. E. Todreas and M. S. Kazimi,** Nuclear Systems I, United States of America: Taylor & Francis, 1993.

APPENDICES

APPENDIX A: Power Fractions Distribution for 5 and 2 channels.
APPENDIX B: Thermodynamic parameters for water at pressure=0.1 kPa.
APPENDIX C: The Moody Chart.

APPENDIX A: Power Fractions Distribution for 5 and 2 channels

Table A.1 : Power fractions for each control volume of each channel, the axial nodes starts from the lowest to the highest location in z direction, used in EUREKA-2/RR model.

Axial node	Channel-1	Channel-2	Channel-3	Channel-4	Channel-5
1	2.58E-03	3.40E-02	3.20E-02	3.10E-02	2.45E-02
2	2.34E-03	3.07E-02	2.84E-02	2.66E-02	2.20E-02
3	2.74E-03	3.56E-02	3.29E-02	3.04E-02	2.64E-02
4	1.45E-03	1.89E-02	1.74E-02	1.61E-02	1.43E-02
5	1.47E-03	1.92E-02	1.76E-02	1.63E-02	1.47E-02
6	1.46E-03	1.91E-02	1.76E-02	1.63E-02	1.49E-02
7	1.43E-03	1.87E-02	1.72E-02	1.60E-02	1.49E-02
8	2.70E-03	3.51E-02	3.23E-02	3.03E-02	2.86E-02
9	2.30E-03	2.99E-02	2.76E-02	2.62E-02	2.56E-02
10	2.43E-03	3.18E-02	2.97E-02	2.93E-02	2.92E-02

Table A.2 : Power fractions for each control volume of each channel, the axial nodes starts from the lowest to the highest location in z direction, used in TM2-RIA model.

Axial node	Hot channel	Average Channel
1	8.897E-04	3.803E-02
2	9.761E-04	4.085E-02
3	1.146E-03	4.663E-02
4	1.298E-03	5.125E-02
5	1.435E-03	5.624E-02
6	1.552E-03	6.087E-02
7	1.640E-03	6.394E-02
8	1.685E-03	6.656E-02
9	1.708E-03	6.763E-02
10	1.704E-03	6.754E-02
11	1.668E-03	6.630E-02
12	1.629E-03	6.408E-02
13	1.523E-03	6.078E-02
14	1.406E-03	5.639E-02
15	1.268E-03	5.112E-02
16	1.093E-03	4.520E-02
17	9.228E-04	3.809E-02
18	8.127E-04	3.404E-02

APPENDIX B: Thermodynamic parameters for water at pressure=0.1 kPa.

Table B.1 : Thermodynamics variables for water at pressure 0.1 kPa, utilized in TM2-RIA.

Temperature (℃)	Enthalpy (kJ/kg)	Density (kg/m^3)	Dynamic Viscosity $(N/m^2 s)$
10	42	999.7	1.31E-6
20	84	998.2	1.00E-6
30	125.8	995.7	0.801E-06
40	167.5	992.3	0.658E-06
50	209.3	988.1	0.553E-06
60	251.2	983.2	0.475E-06
70	293.0	977.8	4.17E-7
80	335.0	971.8	3.68E-7
90	377.0	965.3	3.28E-7
100	419.0	959.1	2.94E-7

APPENDIX C: The Moody Chart.

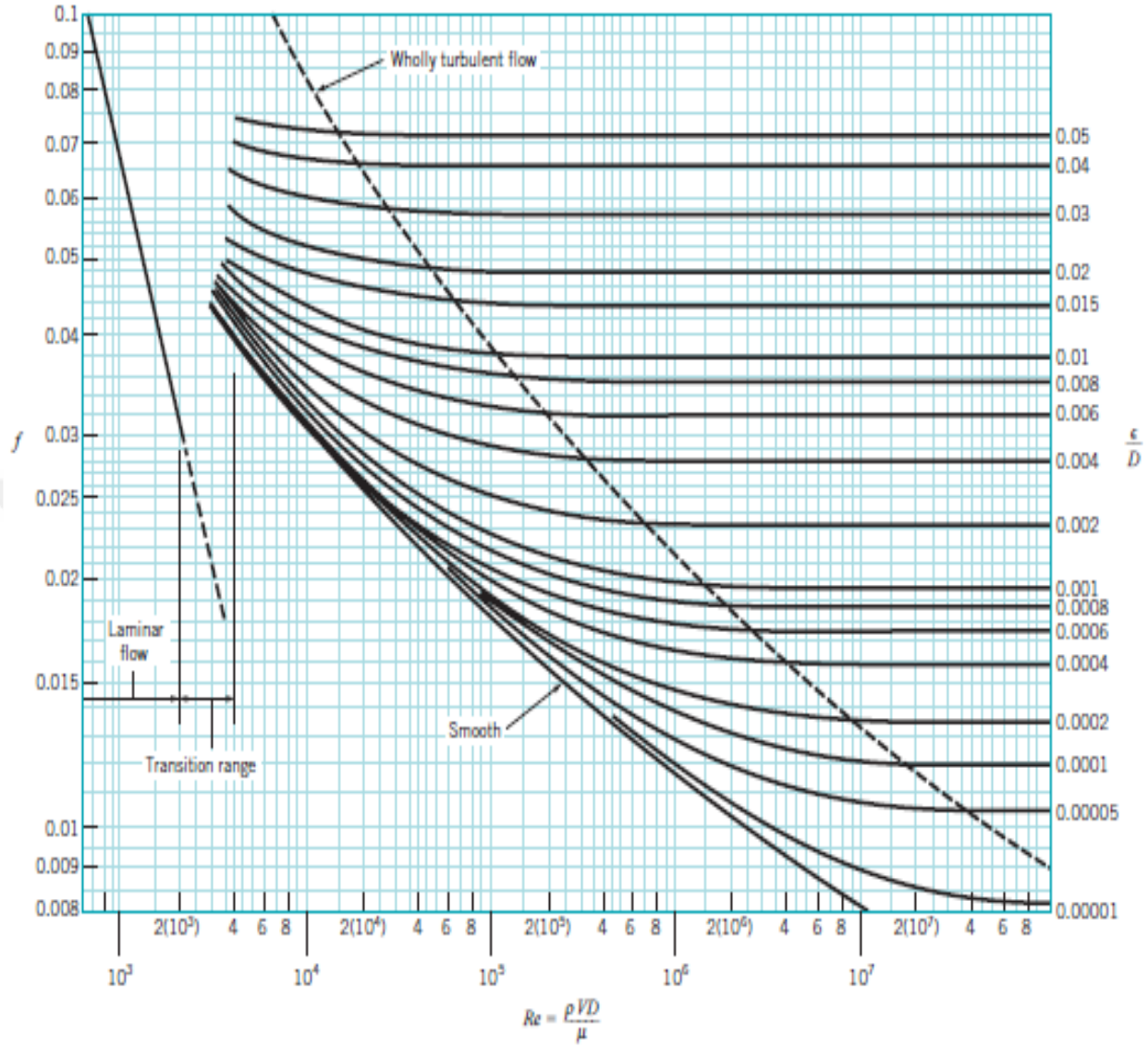

Figure C.1 : Friction factor as a function of Reynolds number and relative roughness for round pipes [55].

CURRICULUM VITAE

Name Surname **:** Mohammad ALLAF

E-Mail **:** allaf17@itu.edu.tr, amer.allaf@yahoo.com

EDUCATION:

B.Sc. **:** 2016, Hacettepe University, Engineering Faculty, Nuclear Engineering Department.

PUBLICATIONS, PRESENTATIONS AND PATENTS ON THE THESIS:

OTHER PUBLICATIONS, PRESENTATIONS AND PATENTS:

- Shahid U., **Allaf M.A.,** Ozkan F. O., Yilmazer A. 2017: Neutronic Modelling of Molten-Salt Reactors, 37th Annual Conference of the Canadian Nuclear Society and 41st Annual CNS/CNA Student Conference proceedings, volume 1, 1369, 4-7 June.
- Gultekin A., **Allaf M.A.,** Colak U., Numerical Investigation of a Single Droplet Impact onto Hot Surface by VOF Method at High Weber Numbers. 27th International Conference Nuclear Energy for New Europe, 10-13 September 2018.
- Kutbay F., **Allaf M.A.,** Senturk Lule S., Colak U., Doppler Broadening Effect on Reactivity Feedback in ITU TRIGA MARK II Research Reactor. 27th International Conference Nuclear Energy for New Europe, 10-13 September 2018.